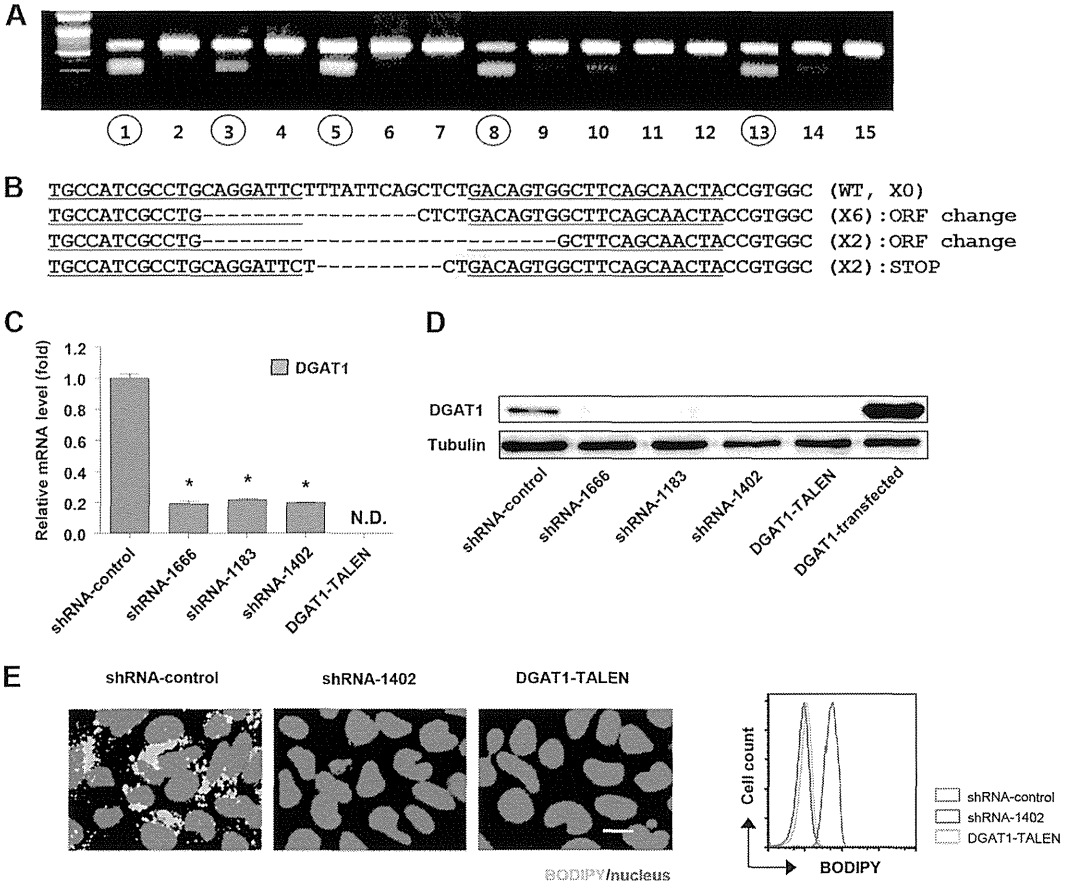

FIG 1 Establishment of DGAT1-silenced cell lines using DGAT1-TALEN or lentivirus vector shRNA DGAT1. (A) Huh-7.5 cells were transfected with plasmids encoding a pair of *DGAT1*-targeting TALENs in combination with the reporter encoding H-2K^k. After the magnetic sorting of cells with TALEN-driven mutations, we analyzed 62 single-cell-derived colonies using the T7E1 assay. The region of the DGAT1 gene containing the TALEN target site was amplified by nested PCR and visualized by agarose gel electrophoresis. Representative data from the T7E1 assay are presented here. Circled numbers indicate clones that were selected for *DGAT1* gene sequencing. (B) DNA sequences of the DGAT1-TALEN cell line. The sequence presented here is part of the *DGAT1* gene of clone 13, one of the clones that are presented in panel A. Zinc finger nuclease recognition sites are underlined, and deleted bases are indicated by dashes. TGA, the premature stop codon, is shaded in gray. Clone 13 has a shifted open reading frame (ORF) or premature stop codon in the *DGAT1* gene. (C) DGAT1 mRNA levels were determined by real-time quantitative PCR in DGAT1-silenced cell lines and standardized to β-actin mRNA levels (n = 3). N.D., not detected. (D) DGAT1 protein expression in DGAT1-silenced cell lines was assessed by immunoblotting. (E) Intracellular lipid droplet staining was performed using the BODIPY lipid probe 493/503 in the control and DGAT1-silenced cell lines. The scale bar represents 20 μm. The right panel represents flow cytometry analyses of the same cell lines.

cells (Fig. 2A). We also quantified intracellular HCV RNA copies and unexpectedly discovered that the intracellular HCV RNA titer was very low in the DGAT1-silenced cell lines (Fig. 2B). Following inoculation of the DGAT1-silenced cell lines with a higher dose of JFH-1, we detected no intracellular HCV core protein by flow cytometry (Fig. 2C).

Next, we transfected the control and DGAT1-silenced cell lines with JFH-1 RNA. As expected from the previous study (11) and loss of intracellular lipid droplets in the DGAT1-silenced cell lines, the production of infectious virions was severely impaired in the DGAT1-silenced cell lines (Fig. 2D). The intracellular HCV RNA copy number was also lower in the DGAT1-silenced cell lines than in the control cell line, with a difference of less than 1 log (Fig. 2E), indicating that HCV RNA replication is slightly impaired in DGAT1-silenced cells. However, this minor decrease is in contrast to the enormous decrease that was observed in the HCVcc inoculation study (Fig. 2B). This finding indicates that another factor is the major cause of the very low intracellular HCV RNA levels in HCVcc-inoculated, DGAT1-silenced cells.

With the hypothesis that HCV entry is defective in DGAT1-silenced cell lines, we evaluated HCV entry using HCVpp of various genotypes. No HCVpp entered the DGAT1-silenced cell lines (Fig. 2F), whereas the control virus pseudoparticles with VSV-G did enter these lines, indicating that HCV entry is impaired in the absence of DGAT1.

Claudin-1 expression is downregulated in DGAT1-silenced cell lines. Because of the impaired HCV entry into DGAT1-silenced cell lines, we investigated the expression of host proteins participating in HCV entry, including tetraspanin CD81 (28), the high-density lipoprotein receptor scavenger receptor class B type I (SR-BI) (29), and two tight junction proteins, claudin-1 (CLDN1) (30) and occludin (OCLN) (31). In the flow cytometric analysis, the expression of CD81, SR-BI, and OCLN in DGAT1-silenced cell lines was well preserved, but that of CLDN1 was markedly diminished (Fig. 3A and B). We observed the downregulation of CLDN1 expression at the mRNA level by real-time quantitative PCR (Fig. 3C). Immunoblotting confirmed the downregulation of CLDN1 expression (Fig. 3D). Notably, CLDN1 expression was

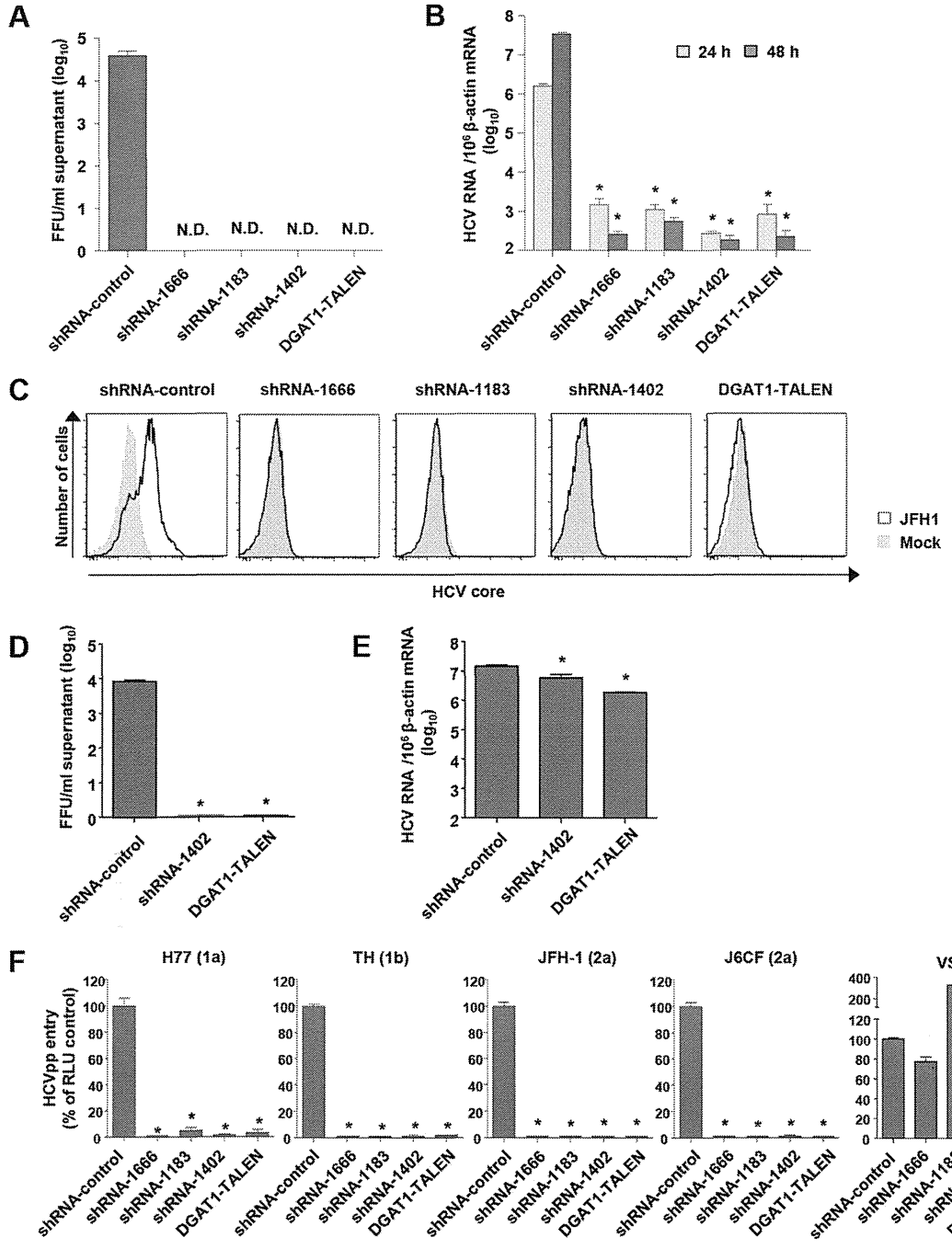

FIG 2 HCV entry into DGAT1-silenced Huh-7.5 cell lines is impaired. (A and B) DGAT1-silenced cell lines were inoculated with JFH-1 HCVcc at a multiplicity of infection (MOI) of 0.1. After 72 h, infectious HCV virions were quantified in culture supernatants by a colorimetric focus-forming assay (19). The data are presented as focus-forming units (FFU) per ml of culture supernatant ($n = 3$) (A). Intracellular HCV RNA levels were determined by real-time quantitative PCR and standardized to β-actin mRNA levels ($n = 3$) (B). (C) DGAT1-silenced cell lines were inoculated with JFH-1 HCVcc at an MOI of 0.5. After 60 h, intracellular HCV core proteins were detected by flow cytometry. Data are representative of two independent experiments. (D and E) DGAT1-silenced cell lines were transfected with 5 μg *in vitro*-transcribed JFH1 RNA. After 72 h, infectious HCV virions were quantified in culture supernatants by a colorimetric focus-forming assay (19). The data are presented as focus-forming units (FFU) per ml of culture supernatant ($n = 3$) (D). Intracellular HCV RNA levels were determined by real-time quantitative PCR and standardized to β-actin mRNA levels ($n = 3$) (E). (F) HCV entry into DGAT1-silenced cell lines was assessed using HCVpp harboring E1 and E2 glycoproteins of various HCV genotypes. Virus pseudoparticles harboring the vesicular stomatitis virus G (VSV-G) envelope glycoprotein were used as a positive control. HCVpp entry was determined by luciferase activity. Data are expressed as percentages of the shRNA-control cell line ($n = 3$). Bar graphs represent means ± SEM. *, $P < 0.001$ compared to the control. N.D., not detected.

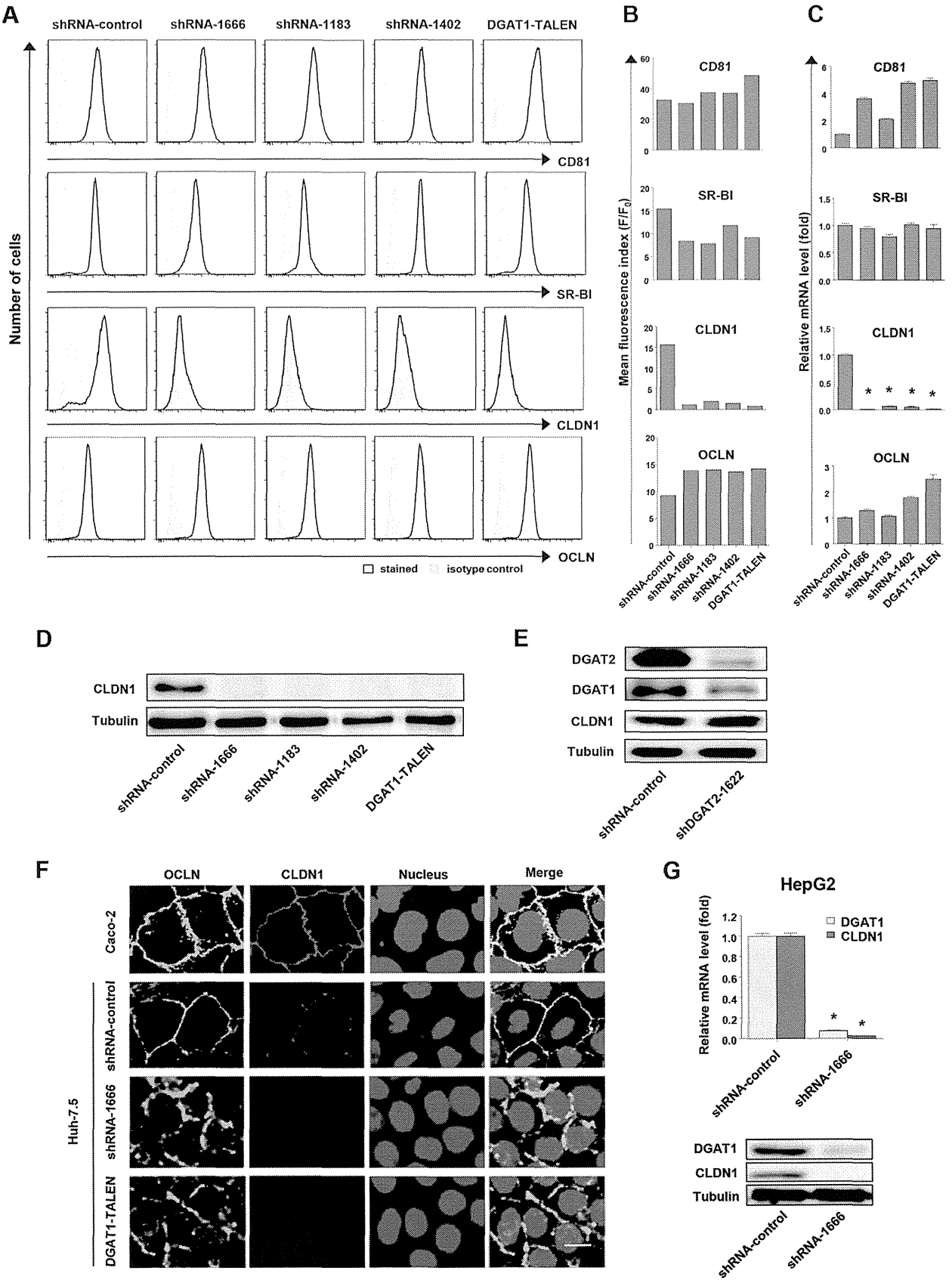

FIG 3 CLDN1 expression is downregulated in DGAT1-silenced cell lines. (A and B) The expression of CD81, SR-B1, CLDN1, and OCLN in DGAT1-silenced cell lines was analyzed by flow cytometry. Histograms are representative of three independent experiments (A), and the mean fluorescence index (F/F_0) of the

not downregulated by the silencing of DGAT2, the other DGAT protein present in human hepatocytes (Fig. 3E). Immunofluorescence staining revealed that CLDN1 expression on the cell membrane was lost in the DGAT1-silenced cells (Fig. 3F). Additionally, a significant proportion of OCLN was localized not only to the cell membrane but also to the cytoplasm in these cells (Fig. 3F). We further confirmed downregulation of CLDN1 at the mRNA and protein levels under DGAT1-silencing conditions in another hepatoma cell line, HepG2, following DGAT1 silencing by lentivirus shRNA transduction (Fig. 3G).

Forced expression of CLDN1 restores HCV entry to DGAT1-silenced cell lines. To verify whether the downregulation of CLDN1 expression led to HCV entry impairment, we transfected DGAT1-silenced cell lines with the *CLDN1* gene and evaluated HCV entry using HCVpp. After 72 h of the transfection, CLDN1 expression was observed by immunoblotting (Fig. 4A) and flow cytometry (Fig. 4B). Importantly, the entry of all of the HCVpp was restored in the CLDN1-expressing DGAT1-silenced cells (Fig. 4C). These results demonstrate that CLDN1 downregulation is responsible for impairment of HCV entry into DGAT1-silenced cells and that the reexpression of CLDN1 is sufficient to restore HCV entry into these cells.

Expression of hepatocyte-specific genes is reduced in DGAT1-silenced cell lines. In DGAT1-silenced cells, we examined the expression of hepatocyte nuclear factor 4α (HNF4α) because this factor has been reported to be associated with CLDN1 expression in mice (32–34). In fact, HNF4α expression was markedly reduced in DGAT1-silenced cell lines at both the mRNA and protein levels (Fig. 5A). HNF4α is a central regulator of hepatocyte differentiation and function (35, 36), and the expression of other hepatocyte-specific genes, such as the albumin and α1-antitrypsin genes, was also decreased in the DGAT1-silenced cells (Fig. 5B), suggesting that their differentiation status had been altered by DGAT1 silencing. However, HNF4α expression was not downregulated by the silencing of DGAT2 (Fig. 5C). We also examined temporal changes in DGAT1, HNF4α, and CLDN1 expression during the establishment of a stable cell line following lentivirus shRNA-DGAT1 transduction into Huh-7.5 cells. DGAT1 expression was silenced at 10 days following transduction, whereas the expression of HNF4α and CLDN1 was preserved (Fig. 5D). HNF4α expression then decreased gradually, followed by a slow decrease in CLDN1 expression. Ultimately, the expression of both HNF4α and CLDN1 was markedly diminished at 45 days following transduction (Fig. 5D).

To verify whether DGAT1 silencing directly caused the downregulation of HNF4α and CLDN1, we transfected shRNA-DGAT1-transduced cells with the shRNA-resistant *DGAT1* gene 10 days after the transduction. Following the transfection, DGAT1 expression was restored, and expression of HNF4α and CLDN1 was maintained (Fig. 6A). In addition, intracellular lipid droplets were restored by transfection (Fig. 6B). Furthermore, HCVpp entry was recovered by the restoration of DGAT1 expression (Fig. 6C). Next, we examined the requirement for the catalytic activity of DGAT1 for the maintenance of CLDN1 and HNF4α expression. We constructed a catalytically inactive *DGAT1* mutant gene (H415A) (11, 37) that was also shRNA resistant. Unlike the catalytically active DGAT1, the catalytically inactive form did not maintain the expression of CLDN1 and HNF4α (Fig. 6D). Collectively, these results indicate that DGAT1 silencing causes HNF4α and CLDN1 downregulation and HCV entry impairment and that the loss of DGAT1 catalytic activity is important in this process.

As HNF4α was reported to upregulate CLDN1 expression in mice (32, 33), we examined whether HNF4α downregulation was responsible for the CLDN1 downregulation that was observed in the DGAT1-silenced cells. In fact, HNF4α bound to the promoter region of human *CLDN1* in the ChIP assay (Fig. 6E and F). However, HNF4α silencing by siRNA (siHNF4α) did not significantly decrease CLDN1 expression (Fig. 6G and H). We also transfected DGAT1-silenced cells with the *HNF4α* gene. For the transfection, we used the gene encoding HNF4α1, which is a major isoform in adult human hepatocytes (38, 39). However, CLDN1 expression was not restored by this transfection (Fig. 6I). Taking these findings together, we conclude that CLDN1 expression is not regulated solely by HNF4α but also by other factors that are influenced by DGAT1 silencing.

Exogenous palmitic acid treatment prevents downregulation of CLDN1 and HNF4α expression after DGAT1 silencing. Considering that DGAT1 regulates intracellular lipid homeostasis (10) and our data showing that intracellular lipid droplets are depleted in DGAT1-silenced cells (Fig. 1E), we hypothesized that CLDN1 downregulation might be attributed to a dysregulation of intracellular fatty acid metabolism. Therefore, we examined the effect of exogenous fatty acid treatment following DGAT1 silencing. We applied BSA-conjugated palmitic acid ($C_{16:0}$) at a low concentration to shRNA-DGAT1-transduced cells 10 days after the transduction and continued the treatment for 17 days. The expression of CLDN1 and HNF4α was preserved by palmitic acid treatment, although DGAT1 expression was silenced (Fig. 7A). Importantly, HCVpp entry was also recovered by palmitic acid treatment (Fig. 7B). These results indicate that altered fatty acid homeostasis in DGAT1-silenced cells is associated with CLDN1 downregulation, which leads to HCV entry impairment.

DISCUSSION

In the present study, we attempted to identify the effects of complete, long-term silencing of DGAT1 on the whole life cycle of HCV in Huh-7.5 cells. We demonstrated that CLDN1 downregulation impairs HCV entry into DGAT1-silenced cell lines and that

histogram is presented (B). F, mean fluorescence intensity (MFI) of specific antibody staining; F_0, MFI of isotype control antibody staining. Data are representative of three independent experiments. (C) mRNA levels of CD81, SR-B1, CLDN1, and OCLN in DGAT1-silenced cell lines were determined by real-time quantitative PCR and standardized to β-actin mRNA levels ($n = 3$). (D) CLDN1 protein expression in DGAT1-silenced cell lines was assessed by immunoblotting. (E) Immunoblot analysis was performed to evaluate CLDN1 expression in the control and DGAT2 knockdown Huh-7.5 cell line after 40 days of shRNA lentiviral transduction. Data are representative of two independent experiments. (F) Immunofluorescence staining was performed using anti-OCLN (green) and anti-CLDN1 (red) in Caco-2, shRNA-control, and DGAT1-silenced Huh-7.5 cell lines, and images were analyzed by confocal microscopy. Merged images are also presented. The scale bar represents 20 μm. (G) A stably DGAT1-silenced HepG2 cell line was established by transduction with a lentivirus harboring shRNA-DGAT1-1666. The mRNA levels of DGAT1 and CLDN1 were determined by real-time quantitative PCR ($n = 3$) (left graph), and the protein expression levels of DGAT1 and CLDN1 were assessed by immunoblotting (right blots). Bar graphs represent means ± SEM. * and **, $P < 0.001$ and $P < 0.01$, respectively, compared to the control.

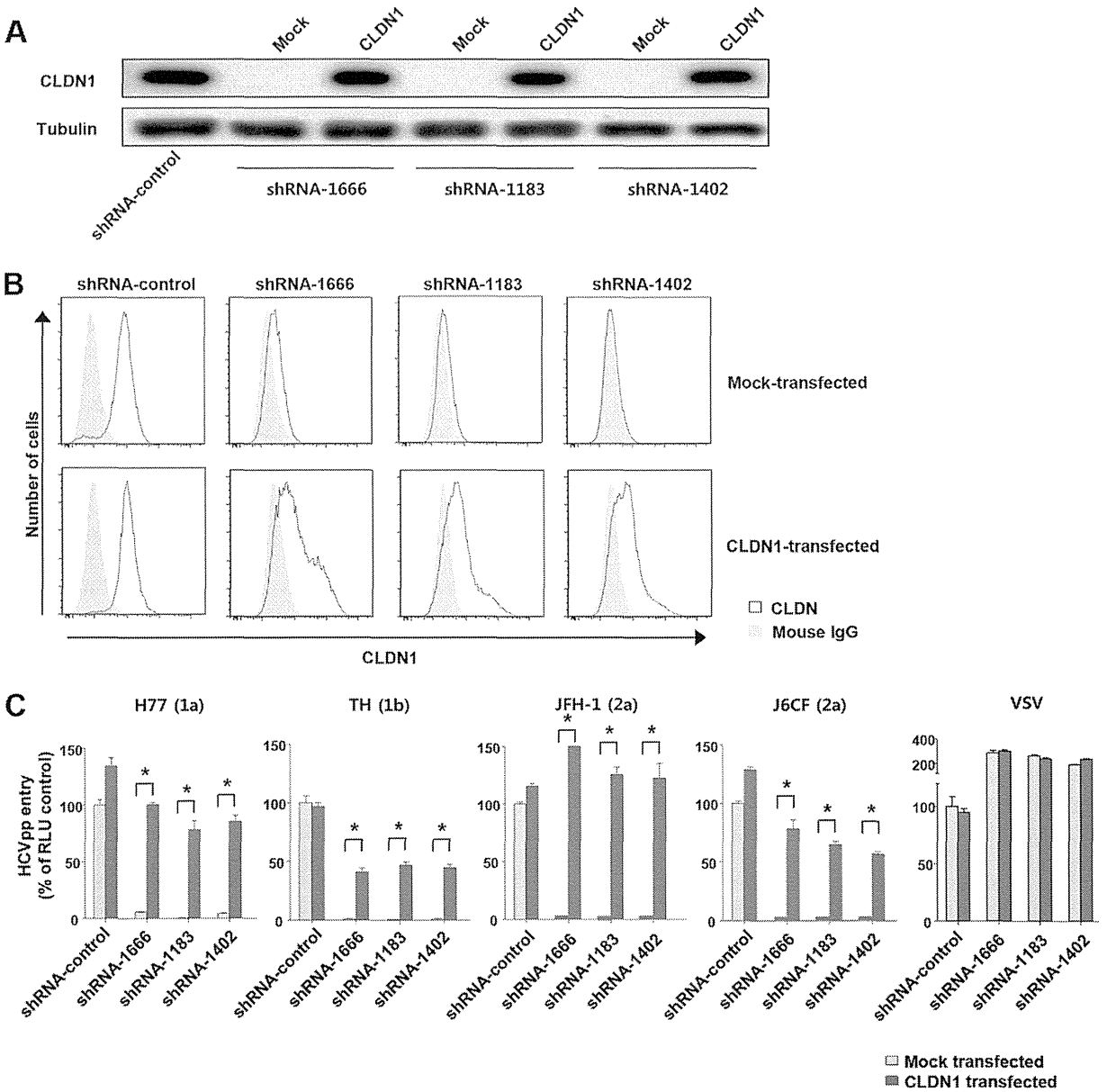

FIG 4 Forced expression of CLDN1 restores HCV entry to DGAT1-silenced cell lines. (A) CLDN1 protein expression was assessed by immunoblotting after mock or CLDN1 transfection of DGAT1-silenced cell lines. (B) Surface expression of CLDN1 was analyzed by flow cytometry after mock or CLDN1 transfection of DGAT1-silenced cell lines. Data are representative of three independent experiments. (C) HCV entry was assessed after mock or CLDN1 transfection of DGAT1-silenced cell lines using HCVpp of various genotypes. Virus pseudoparticles harboring the VSV-G envelope glycoprotein served as a positive control. HCVpp entry was determined by luciferase activity. Data are expressed as percentages of the shRNA-control cell line ($n = 4$). The statistical analysis was conducted for differences between the mock-transfected and CLDN1-transfected cells. Bar graphs represent means ± SEM. *, $P < 0.001$.

this effect is associated with altered fatty acid homeostasis. However, these findings were made using the Huh-7.5 human hepatoma cell line and need to be confirmed in primary human hepatocytes.

One of the main roles of DGAT1 is in catalyzing the final step of triglyceride biosynthesis (5, 6). However, studies of knockout mice have shown that DGAT1 deficiency does not result in elevated levels of diacylglycerol or acyl coenzyme A (acyl-CoA) in the liver, heart, muscle, and adipose tissue following the ingestion of high-fat diets (7, 40). These data suggest that DGAT1 does not simply catalyze the final step of triglyceride biosynthesis but is involved in the regulation of intracellular lipid homeostasis. In fact, DGAT1 recycles the products of triglyceride hydrolysis, which are partial glycerides, for triglyceride synthesis. In addition, DGAT1 inhibition decreases the intracellular lipid pool comprised of triglycerides, partial glycerides, and free fatty acids in human liver-derived cells (10, 41). In the present study, a low-dose exogenous palmitic acid treatment prevented the down-regulation of CLDN1 and HNF4α expression in DGAT1-silenced cells. These results show that expression of CLDN1 and HNF4α is regulated by altered intracellular lipid homeostasis in DGAT1-silenced cells and that the restoration of intracellular fatty acid levels by exogenous palmitic acid rescued CLDN1 and HNF4α expression.

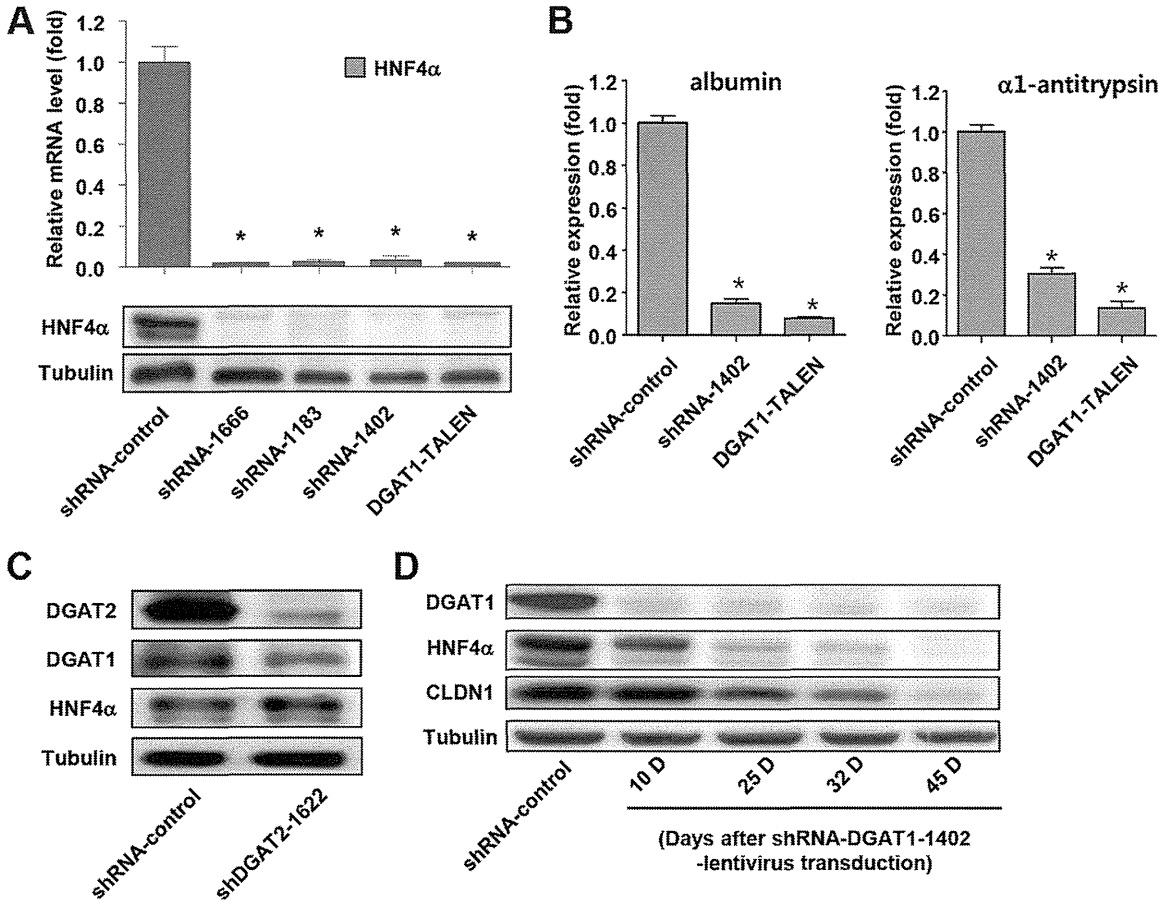

FIG 5 Expression of hepatocyte-specific genes is reduced in DGAT1-silenced cell lines. (A) HNF4α mRNA levels in DGAT1-silenced cell lines were determined by real-time quantitative PCR ($n = 3$) (upper graph), and HNF4α protein expression was assessed by immunoblotting (lower blots). (B) mRNA expression of representative hepatic differentiation markers in control and DGAT1-silenced cell lines. Data are standardized to β-actin mRNA levels ($n = 3$). Bar graphs represent means ± SEM. *, $P < 0.001$ compared to the control. (C) Immunoblot analysis was performed to evaluate HNF4α expression in control and DGAT2 knockdown Huh-7.5 cell lines after 40 days of lentivirus shRNA transduction. Data are representative of two independent experiments. (D) Huh-7.5 cells were transduced with lentivirus harboring shRNA-DGAT1-1402, and temporal changes in protein expression were examined during the establishment of a stable cell line. The cell pellets were harvested at days 10, 25, 32, and 45 after transduction and subjected to immunoblot analyses to detect DGAT1, HNF4α, and CLDN1. Data are representative of two independent experiments.

We also made a DGAT2-silenced cell line in this study. However, the expression of CLDN1 and HNF4α was not downregulated in the DGAT2-silenced cells (Fig. 3E and 5C). DGAT2 also catalyzes the final step of triglyceride synthesis, but recent reports suggest that DGAT1 and DGAT2 play different roles in human hepatocytes (10). DGAT2 is involved in the *de novo* synthesis of triglycerides, whereas DGAT1 functions in the reesterification of partial glycerides that are generated by intracellular lipolysis. Moreover, DGAT2 encompasses 30% of the total DGAT activity in human hepatocytes, whereas DGAT1 contributes the other 70% (10).

HNF4α is a central regulator of hepatocyte differentiation and function (33, 34) and is a major transcription factor that regulates the expression of genes that are involved in lipid homeostasis (42). HNF4α is also known to regulate the expression of proteins that are required for hepatic and intestinal tight junction assembly, including CLDN1, in mice (30–32). A recent study demonstrated the binding of HNF4α to the CLDN1 gene by an electrophoretic mobility shift assay and ChIP assay of the mouse fetal liver (30). In accordance with this previous report, our present data showed that HNF4α bound to the promoter region of human *CLDN1* in a ChIP assay (Fig. 6E and F). However, HNF4α silencing did not significantly decrease CLDN1 expression (Fig. 6G and H), and *HNF4α1* transfection did not restore CLDN1 expression in DGAT1-silenced cells (Fig. 6I). Taking these findings together, we conclude that CLDN1 expression is not regulated solely by HNF4α but also by other factors that are influenced by DGAT1 silencing.

A previous study has shown that DGAT1 is involved in the assembly of HCV by facilitating the trafficking of the HCV core protein to the lipid droplet (11). The authors suppressed DGAT1 activity by using a DGAT1 inhibitor or silenced DGAT1 expression by shRNA, but they observed no impairment of HCV entry to Huh-7.5 cells. The discrepancy between the studies may be explained by the duration of DGAT1 inhibition or silencing. The earlier study involved the use of the DGAT inhibitor for a short duration of approximately 72 h. In contrast, we used stable DGAT1-silenced cell lines to study the long-term effects of DGAT1 silencing. In fact, CLDN1 expression decreased gradually in shRNA-DGAT1-transduced cells and was markedly downregu-

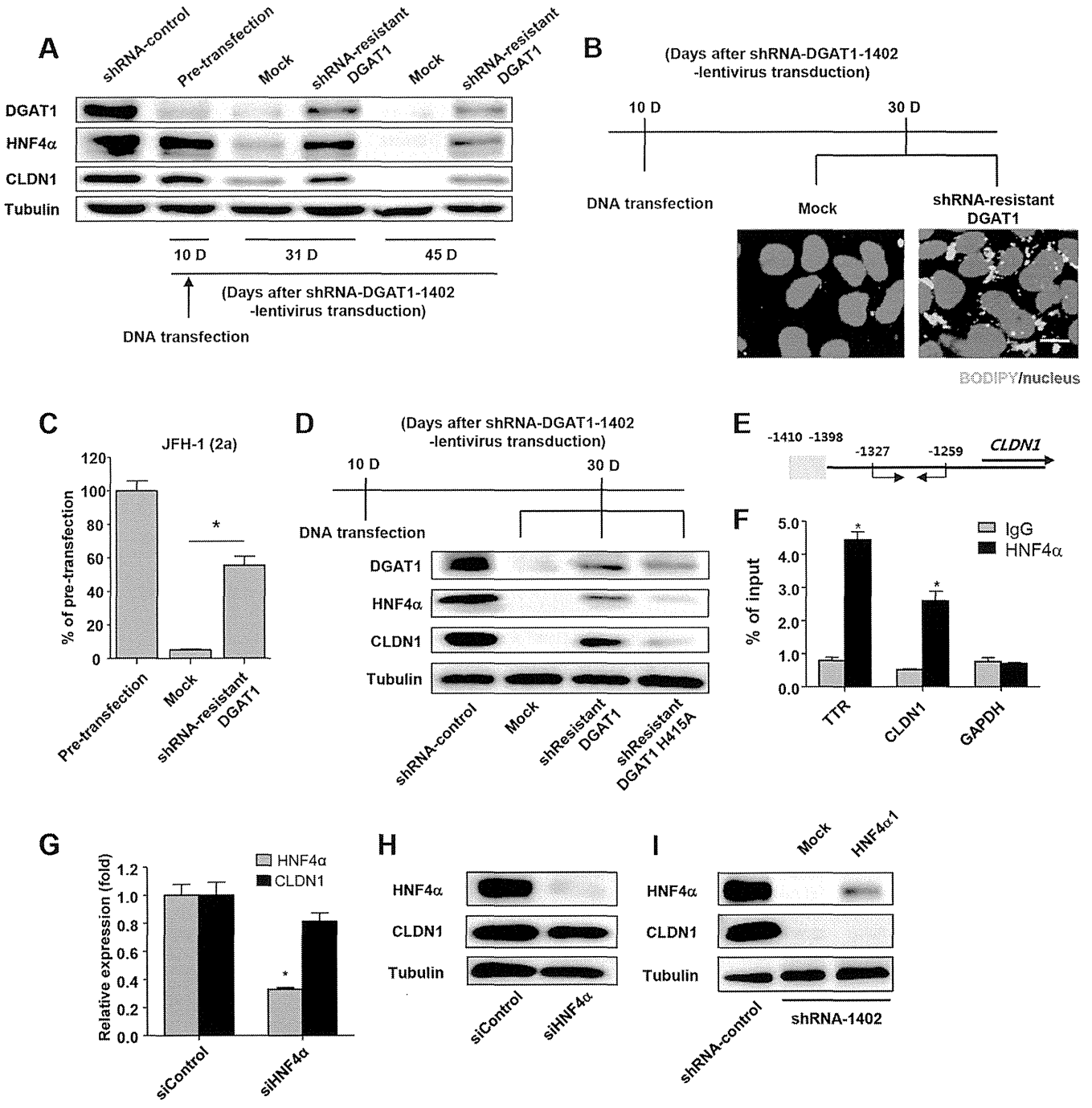

FIG 6 Catalytically active DGAT1 is responsible for maintaining CLDN1 expression and the hepatocyte-specific phenotype in Huh-7.5 cells. (A) An shRNA-1402-resistant *DGAT1* gene was constructed by introducing 6 point mutations into the sequence that is recognized by the shRNA-1402 oligonucleotide without altering the amino acid sequence. The shRNA-1402-resistant *DGAT1* gene was transfected into shRNA-DGAT1-1402-harboring cells 10 days after transduction, and temporal changes in protein expression were examined. The cell pellets were harvested at days 10, 31, and 45 after transduction with lentivirus harboring shRNA-DGAT1-1402 (days 0, 21, and 35 after the shRNA-1402-resistant DGAT1 transfection) and were subjected to immunoblot analysis to detect DGAT1, HNF4α, and CLDN1. Data are representative of two independent experiments. (B) Intracellular lipid droplet staining was performed using the BODIPY lipid probe 493/503 in cells that had been transfected with mock or shRNA-resistant DGAT1. The scale bar represents 20 μm. (C) HCV entry into DGAT1-silenced cell lines was assessed after mock or shRNA-resistant DGAT1 transfection using JFH1 HCVpp. Data are expressed as percentages of the pretransfected cell line ($n = 3$). Bar graphs represent means ± SEM. *, $P < 0.001$. (D) Immunoblot analysis of DGAT1-silenced cell lines harboring a catalytically active or inactive DGAT1 gene was performed. A catalytically inactive DGAT1-encoding plasmid was constructed by site-directed mutagenesis, replacing the histidine residue at position 415 (encoded by CAU) with alanine (encoded by GCU), and the catalytically inactive *DGAT1* gene was also shRNA resistant. We confirmed the sequence of the mutated construct, which was then used to transfect Huh-7.5 cells on 10 days after DGAT1 silencing. Data are representative of two independent experiments. (E, F) The chromatin immunoprecipitation assay was performed using anti-HNF4α antibody. In the schematic of the CLDN1 promoters, the putative HNF4α binding site is shaded in gray, and the positions of the primers for real-time qPCR are designated with arrows (E). Real-time qPCR analysis was performed using DNA precipitated by rabbit anti-HNF4α (clone number H171) (Santa Cruz Biotechnology, Inc.) or IgG. Transthyretin (TTR) was used as a positive control (F). *, $P < 0.01$ ($n = 3$). (G) Real-time qPCR analysis of HNF4α and CLDN1 expression in the Huh-7.5 cell line was conducted after siHNF4α treatment. Data are standardized to β-actin mRNA levels ($n = 3$). Bar graphs represent means ± SEM. *, $P < 0.001$. (H) Immunoblot analysis of HNF4α and CLDN1 in the Huh-7.5 cell line was performed after siHNF4α treatment. Data are representative of two independent experiments. (I) Immunoblot analysis of HNF4α and CLDN1 in DGAT1-silenced cell lines was performed at 72 h after transfection with HNF4α1 plasmid. Data are representative of two independent experiments.

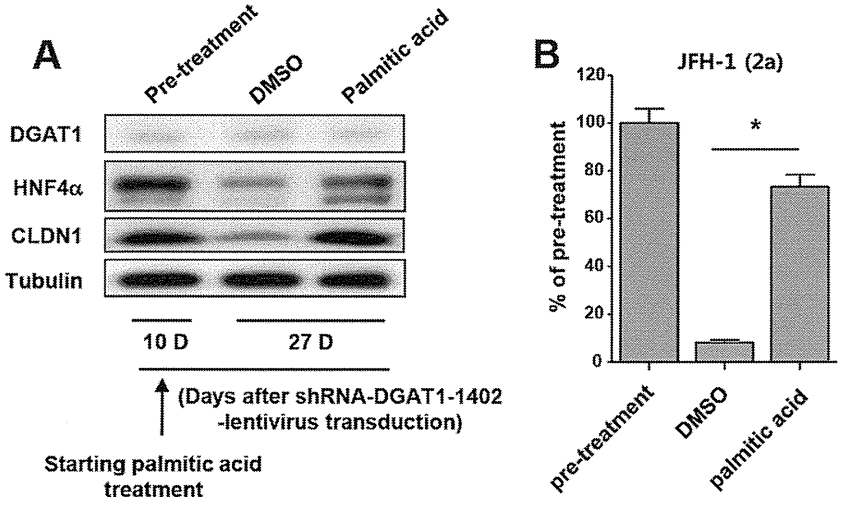

FIG 7 Exogenous palmitic acid treatment prevents downregulation of CLDN1 and HNF4α expression after DGAT1 silencing. (A) From day 10 after transduction with lentiviruses harboring shRNA-DGAT1-1402, the transduced cells were cultured in medium that had been supplemented with 10% charcoal-stripped fetal bovine serum and 1% bovine serum albumin with either 50 μM palmitic acid or DMSO. The cell pellets were harvested at days 10 and 27 after transduction (days 0 and 17 after the palmitic acid treatment) and subjected to immunoblot analysis to detect DGAT1, HNF4α, and CLDN1. Data are representative of two independent experiments. (B) HCV entry (of JFH1 HCVpp) into DGAT1-silenced cell lines was assessed after DMSO or palmitic acid treatment. Data are expressed as percentages of the values for the pretreatment cell lines ($n = 3$). Bar graphs represent means ± SEM. *, $P < 0.001$.

lated only after long-term culturing for over 45 days (Fig. 5D). In the present study, we also knocked out the *DGAT1* gene by using the TALEN technique to silence DGAT1 expression completely and found no DGAT1 expression in the DGAT1-TALEN cell line (Fig. 1C and D). Interestingly, DGAT1-TALEN transfection facilitated CLDN1 downregulation compared to shRNA-DGAT1 transduction in the process of stable cell line establishment (data not shown). CLDN1 downregulation may be induced only by the complete silencing of DGAT1, which could be achieved by a long-term culture of shRNA-DGAT1-transduced cells or by highly efficient silencing with DGAT1-TALEN.

In the present study, we found that HCV RNA replication was also slightly impaired in DGAT1-silenced cell lines (Fig. 2E). This impairment can be partially attributed to the loss of lipid droplets in these cells (Fig. 1E). In fact, recent studies have emphasized the association of lipid droplets and HCV RNA replication (43). Further research is required to clarify the manner by which HCV RNA replication is influenced by intracellular fatty acid homeostasis.

In conclusion, our data demonstrate that complete, long-term silencing of DGAT1 causes CLDN1 downregulation and thus inhibits HCV entry and that CLDN1 downregulation is associated with altered fatty acid homeostasis in the absence of DGAT1. Future research is needed to elucidate the exact mechanisms and consequences of CLDN1 downregulation in DGAT1-silenced hepatocytes.

ACKNOWLEDGMENTS

This work was supported by a National Agenda Project grant from the Korea Research Council of Fundamental Science and Technology (NTM1311423), the Korea Research Institute for Bioscience and Biotechnology (KRIBB) Initiative Program (KGM3121423), and by the Project of Global Ph.D. Fellowship (NRF-2012H1A2A1012809, to P.S.S.) through the National Research Foundation of Korea (NRF) funded by the Ministry of Science, ICT, and Future Planning of Korea. A.M. and T.K. were supported by a grant-in-aid from the Japan Society for the Promotion of Science and from the Ministry of Health, Labor, and Welfare of Japan. This work was partly supported by the KAIST (Korea Advanced Institute of Science and Technology) Future Systems Healthcare Project from the Ministry of Science, ICT, and Future Planning of Korea.

REFERENCES

1. **Lavanchy D.** 2011. Evolving epidemiology of hepatitis C virus. Clin. Microbiol. Infect. **17**:107–115. http://dx.doi.org/10.1111/j.1469-0691.2010.03432.x.
2. **Liang TJ, Ghany MG.** 2013. Current and future therapies for hepatitis C virus infection. N. Engl. J. Med. **368**:1907–1917. http://dx.doi.org/10.1056/NEJMra1213651.
3. **Aloia AL, Locarnini S, Beard MR.** 2012. Antiviral resistance and direct-acting antiviral agents for HCV. Antivir. Ther. **17**:1147–1162. http://dx.doi.org/10.3851/IMP2426.
4. **Zeisel MB, Lupberger J, Fofana I, Baumert TF.** 2013. Host-targeting agents for prevention and treatment of chronic hepatitis C—perspectives and challenges. J. Hepatol. **58**:375–384. http://dx.doi.org/10.1016/j.jhep.2012.09.022.
5. **Cases S, Smith SJ, Zheng YW, Myers HM, Lear SR, Sande E, Novak S, Collins C, Welch CB, Lusis AJ, Erickson SK, Farese RV, Jr.** 1998. Identification of a gene encoding an acyl CoA:diacylglycerol acyltransferase, a key enzyme in triacylglycerol synthesis. Proc. Natl. Acad. Sci. U. S. A. **95**:13018–13023. http://dx.doi.org/10.1073/pnas.95.22.13018.
6. **Yen CL, Stone SJ, Koliwad S, Harris C, Farese RV, Jr.** 2008. Thematic review series: glycerolipids. DGAT enzymes and triacylglycerol biosynthesis. J. Lipid Res. **49**:2283–2301. http://dx.doi.org/10.1194/jlr.R800018-JLR200.
7. **Smith SJ, Cases S, Jensen DR, Chen HC, Sande E, Tow B, Sanan DA, Raber J, Eckel RH, Farese RV, Jr.** 2000. Obesity resistance and multiple mechanisms of triglyceride synthesis in mice lacking Dgat. Nat. Genet. **25**:87–90. http://dx.doi.org/10.1038/75651.
8. **Devita RJ, Pinto S.** 3 September 2013. Current status of the research and development of diacylglycerol O-acyltransferase 1 (DGAT1) inhibitors. J. Med. Chem. http://dx.doi.org/10.1021/jm4007033.
9. **Haas JT, Winter HS, Lim E, Kirby A, Blumenstiel B, DeFelice M, Gabriel S, Jalas C, Branski D, Grueter CA, Toporovski MS, Walther TC, Daly MJ, Farese RV, Jr.** 2012. DGAT1 mutation is linked to a congenital diarrheal disorder. J. Clin. Invest. **122**:4680–4684. http://dx.doi.org/10.1172/JCI64873.
10. **Wurie HR, Buckett L, Zammit VA.** 2012. Diacylglycerol acyltransferase 2 acts upstream of diacylglycerol acyltransferase 1 and utilizes nascent diglycerides and de novo synthesized fatty acids in HepG2 cells. FEBS J. **279**:3033–3047. http://dx.doi.org/10.1111/j.1742-4658.2012.08684.x.

11. Herker E, Harris C, Hernandez C, Carpentier A, Kaehlcke K, Rosenberg AR, Farese RV, Jr, Ott M. 2010. Efficient hepatitis C virus particle formation requires diacylglycerol acyltransferase-1. Nat. Med. 16:1295–1298. http://dx.doi.org/10.1038/nm.2238.
12. Camus G, Herker E, Modi AA, Haas JT, Ramage HR, Farese RV, Jr, Ott M. 2013. Diacylglycerol acyltransferase-1 localizes hepatitis C virus NS5A protein to lipid droplets and enhances NS5A interaction with the viral capsid core. J. Biol. Chem. 288:9915–9923. http://dx.doi.org/10.1074/jbc.M112.434910.
13. Blight KJ, McKeating JA, Rice CM. 2002. Highly permissive cell lines for subgenomic and genomic hepatitis C virus RNA replication. J. Virol. 76:13001–13014. http://dx.doi.org/10.1128/JVI.76.24.13001-13014.2002.
14. Kato T, Miyamoto M, Furusaka A, Date T, Yasui K, Kato J, Matsushima S, Komatsu T, Wakita T. 2003. Processing of hepatitis C virus core protein is regulated by its C-terminal sequence. J. Med. Virol. 69:357–366. http://dx.doi.org/10.1002/jmv.10297.
15. Lindenbach BD, Evans MJ, Syder AJ, Wölk B, Tellinghuisen TL, Liu CC, Maruyama T, Hynes RO, Burton DR, McKeating JA, Rice CM. 2005. Complete replication of hepatitis C virus in cell culture. Science 309:623–626. http://dx.doi.org/10.1126/science.1114016.
16. Wakita T, Pietschmann T, Kato T, Date T, Miyamoto M, Zhao Z, Murthy K, Habermann A, Kräusslich HG, Mizokami M, Bartenschlager R, Liang TJ. 2005. Production of infectious hepatitis C virus in tissue culture from a cloned viral genome. Nat. Med. 11:791–796. http://dx.doi.org/10.1038/nm1268.
17. Zhong J, Gastaminza P, Cheng G, Kapadia S, Kato T, Burton DR, Wieland SF, Uprichard SL, Wakita T, Chisari FV. 2005. Robust hepatitis C virus infection in vitro. Proc. Natl. Acad. Sci. U. S. A. 102:9294–9299. http://dx.doi.org/10.1073/pnas.0503596102.
18. Park J, Kang W, Ryu SW, Kim WI, Chang DY, Lee DH, Park DY, Choi Y-H, Choi K, Shin E-C, Choi C. 2012. Hepatitis C virus infection enhances TNFalpha-induced cell death via suppression of NF-kappaB. Hepatology 56:831–840. http://dx.doi.org/10.1002/hep.25726.
19. Kang W, Shin EC. 2012. Colorimetric focus-forming assay with automated focus counting by image analysis for quantification of infectious hepatitis C virions. PLoS One 7:e43960. http://dx.doi.org/10.1371/journal.pone.0043960.
20. Bartosch B, Dubuisson J, Cosset FL. 2003. Infectious hepatitis C virus pseudo-particles containing functional E1-E2 envelope protein complexes. J. Exp. Med. 197:633–642. http://dx.doi.org/10.1084/jem.20021756.
21. Matsumura T, Kato T, Sugiyama N, Tasaka-Fujita M, Murayama A, Masaki T, Wakita T, Imawari M. 2012. 25-Hydroxyvitamin D3 suppresses hepatitis C virus production. Hepatology 56:1231–1239. http://dx.doi.org/10.1002/hep.25763.
22. Kim Y, Kweon J, Kim A, Chon JK, Yoo JY, Kim HJ, Kim S, Lee C, Jeong E, Chung E, Kim D, Lee MS, Go EM, Song HJ, Kim H, Cho N, Bang D, Kim S, Kim JS. 2013. A library of TAL effector nucleases spanning the human genome. Nat. Biotechnol. 31:251–258. http://dx.doi.org/10.1038/nbt.2517.
23. Kim H, Kim MS, Wee G, Lee CI, Kim H, Kim JS. 2013. Magnetic separation and antibiotics selection enable enrichment of cells with ZFN/TALEN-induced mutations. PLoS One 8:e56476. http://dx.doi.org/10.1371/journal.pone.0056476.
24. Doyon Y, Choi VM, Xia DF, Vo TD, Gregory PD, Holmes MC. 2010. Transient cold shock enhances zinc-finger nuclease-mediated gene disruption. Nat. Methods 7:459–460. http://dx.doi.org/10.1038/nmeth.1456.
25. Takeuchi T, Katsume A, Tanaka T, Abe A, Inoue K, Tsukiyama-Kohara K, Kawaguchi R, Tanaka S, Kohara M. 1999. Real-time detection system for quantification of hepatitis C virus genome. Gastroenterology 116:636–642. http://dx.doi.org/10.1016/S0016-5085(99)70185-X.
26. Fang B, Mane-Padros D, Bolotin E, Jiang T, Sladek FM. 2012. Identification of a binding motif specific to HNF4 by comparative analysis of multiple nuclear receptors. Nucleic Acids Res. 40:5343–5356. http://dx.doi.org/10.1093/nar/gks190.
27. Runkle EA, Rice SJ, Qi J, Masser D, Antonetti DA, Winslow MM, Mu D. 2012. Occludin is a direct target of thyroid transcription factor-1 (TTF-1/NKX2–1). J. Biol. Chem. 287:28790–287801. http://dx.doi.org/10.1074/jbc.M112.367987.
28. Pileri P, Uematsu Y, Campagnoli S, Galli G, Falugi F, Petracca R, Weiner AJ, Houghton M, Rosa D, Grandi G, Abrignani S. 1998. Binding of hepatitis C virus to CD81. Science 282:938–941. http://dx.doi.org/10.1126/science.282.5390.938.
29. Scarselli E, Ansuini H, Cerino R, Roccasecca RM, Acali S, Filocamo G, Traboni C, Nicosia A, Cortese R, Vitelli A. 2002. The human scavenger receptor class B type I is a novel candidate receptor for the hepatitis C virus. EMBO J. 21:5017–5025. http://dx.doi.org/10.1093/emboj/cdf529.
30. Evans MJ, von Hahn T, Tscherne DM, Syder AJ, Panis M, Wölk B, Hatziioannou T, McKeating JA, Bieniasz PD, Rice CM. 2007. Claudin-1 is a hepatitis C virus co-receptor required for a late step in entry. Nature 446:801–805. http://dx.doi.org/10.1038/nature05654.
31. Ploss A, Evans MJ, Gaysinskaya VA, Panis M, You H, de Jong YP, Rice CM. 2009. Human occludin is a hepatitis C virus entry factor required for infection of mouse cells. Nature 457:882–886. http://dx.doi.org/10.1038/nature07684.
32. Battle MA, Konopka G, Parviz F, Gaggl AL, Yang C, Sladek FM, Duncan SA. 2006. Hepatocyte nuclear factor 4alpha orchestrates expression of cell adhesion proteins during the epithelial transformation of the developing liver. Proc. Natl. Acad. Sci. U. S. A. 103:8419–8424. http://dx.doi.org/10.1073/pnas.0600246103.
33. Walesky C, Gunewardena S, Terwilliger EF, Edwards G, Borude P, Apte U. 2013. Hepatocyte-specific deletion of hepatocyte nuclear factor-4α in adult mice results in increased hepatocyte proliferation. Am. J. Physiol. Gastrointest. Liver Physiol. 304:G26–G37. http://dx.doi.org/10.1152/ajpgi.00064.2012.
34. Zhong W, Zhao Y, McClain CJ, Kang YJ, Zhou Z. 2010. Inactivation of hepatocyte nuclear factor-4α mediates alcohol-induced downregulation of intestinal tight junction proteins. Am. J. Physiol. Gastrointest. Liver Physiol. 299:G643–G651. http://dx.doi.org/10.1152/ajpgi.00515.2009.
35. Bolotin E, Liao H, Ta TC, Yang C, Hwang-Verslues W, Evans JR, Jiang T, Sladek FM. 2010. Integrated approach for the identification of human hepatocyte nuclear factor 4alpha target genes using protein binding microarrays. Hepatology 51:642–653. http://dx.doi.org/10.1002/hep.23357.
36. Tirona RG, Lee W, Leake BF, Lan LB, Cline CB, Lamba V, Parviz F, Duncan SA, Inoue Y, Gonzalez FJ, Schuetz EG, Kim RB. 2003. The orphan nuclear receptor HNF4alpha determines PXR- and CAR-mediated xenobiotic induction of CYP3A4. Nat. Med. 9:220–224. http://dx.doi.org/10.1038/nm815.
37. Hofmann K. 2000. A superfamily of membrane-bound O-acyltransferases with implications for wnt signaling. Trends Biochem. Sci. 25:111–112. http://dx.doi.org/10.1016/S0968-0004(99)01539-X.
38. Nakhei H, Lingott A, Lemm I, Ryffel GU. 1998. An alternative splice variant of the tissue specific transcription factor HNF4alpha predominates in undifferentiated murine cell types. Nucleic Acids Res. 26:497–504. http://dx.doi.org/10.1093/nar/26.2.497.
39. Babeu JP, Boudreau F. 2014. Hepatocyte nuclear factor 4-alpha involvement in liver and intestinal inflammatory networks. World J. Gastroenterol. 20:22–30. http://dx.doi.org/10.3748/wjg.v20.i1.22.
40. Liu L, Yu S, Khan RS, Ables GP, Bharadwaj KG, Hu Y, Huggins LA, Eriksson JW, Buckett LK, Turnbull AV, Ginsberg HN, Blaner WS, Huang LS, Goldberg IJ. 2011. DGAT1 deficiency decreases PPAR expression and does not lead to lipotoxicity in cardiac and skeletal muscle. J. Lipid Res. 52:732–744. http://dx.doi.org/10.1194/jlr.M011395.
41. Wurie HR, Buckett L, Zammit VA. 2011. Evidence that diacylglycerol acyltransferase 1 (DGAT1) has dual membrane topology in the endoplasmic reticulum of HepG2 cells. J. Biol. Chem. 286:36238–36247. http://dx.doi.org/10.1074/jbc.M111.251900.
42. Hayhurst GP, Lee YH, Lambert G, Ward JM, Gonzalez FJ. 2001. Hepatocyte nuclear factor 4alpha (nuclear receptor 2A1) is essential for maintenance of hepatic gene expression and lipid homeostasis. Mol. Cell. Biol. 21:1393–1403. http://dx.doi.org/10.1128/MCB.21.4.1393-1403.2001.
43. Tanaka T, Kuroda K, Ikeda M, Wakita T, Kato N, Makishima M. 2013. Hepatitis C virus NS4B targets lipid droplets through hydrophobic residues in the amphipathic helices. J. Lipid Res. 54:881–892. http://dx.doi.org/10.1194/jlr.M026443.

Supplementary Figure 1

Silenced genes	Cell line	Oligonucleotide sequence
DGAT1	shRNA-1666	CCGGCGACTACTACGTGCTCAACTACTCGAGTAGTTGAGCACGTAGTAGTCGTTTTTG
	shRNA-1183	CCGGCATGGACTACTCACGCATCATCTCGAGATGATGCGTGAGTAGTCCATGTTTTTG
	shRNA-1402	CCGGCAGACACTTCTACAAGCCCATCTCGAGATGGGCTTGTAGAAGTGTCTGTTTTTG
DGAT2	shRNA-1622	CCGGGTTCTAGGTGGTGGCTAAATCCTCGAGGATTTAGCCACCACCTAGAACTTTTTTG

Sequences of three different shRNA-DGAT1 and shRNA-DGAT2 oligonucleotides.

Underlined parts are the sequences recognized by respective mRNAs.

The International Journal of Biochemistry & Cell Biology 53 (2014) 329–333

Contents lists available at ScienceDirect

The International Journal of Biochemistry & Cell Biology

journal homepage: www.elsevier.com/locate/biocel

Cells in focus

Dendritic cell subsets involved in type I IFN induction in mouse measles virus infection models

Hiromi Takaki *, Hiroyuki Oshiumi, Misako Matsumoto, Tsukasa Seya *

Department of Microbiology and Immunology, Hokkaido University Graduate School of Medicine, Kita-ku, Sapporo 060-8638, Japan

ARTICLE INFO

Article history:
Received 20 March 2014
Received in revised form 28 April 2014
Accepted 1 May 2014
Available online 4 June 2014

Keywords:
Dendritic cells
Measles virus
Mouse model
Type I interferon (IFN)
Immune suppression

ABSTRACT

Measles caused by measles virus (MV) infection remains important in child mortality. Although the natural host of MV is human, mouse models expressing MV entry receptors (human CD46, CD150) and disrupting the interferon (IFN) pathways work for investigating immune responses during early MV infection *in vivo*. Dendritic cells (DCs) are primary targets for MV in the mouse models and are efficiently infected with several MV strains in the respiratory tract *in vivo*. However, questions remain about what kind of DC in a variety of DC subsets is involved in initial MV infection and how the RNA sensors evoke circumventing signals against MV in infected DCs. Since type I IFN-inducing pathways are a pivotal defense system that leads to the restriction of systemic viral infection, we have generated CD150-transgenic mice with disrupting each of the IFN-inducing pathway, and clarified that DC subsets had subset-specific IFN-inducing systems, which critically determined the DC's differential susceptibility to MV.

1. Introduction

The pathogenic measles virus (MV) causes measles in infants. The MV genome is a nonsegmented negative single-stranded RNA consisting of six genes that encode the nucleocapsid (N), phosphoprotein (P), matrix (M), fusion (F), hemagglutinin (H), and large (L) proteins. The P gene encodes P protein and the nonstructural V and C proteins. Although the nonstructural V and C proteins of wild type (WT) strains of MV are important in suppressing the host interferon (IFN) response in human cells (Gerlier and Valentin, 2009), WT strains of MV are less able to suppress type I IFN production in murine cells than in human cells (Shingai et al., 2005), suggesting that V and C proteins are relatively ineffective suppressors for IFN response in murine cells.

CD46 (also called MCP) was first identified as an MV entry receptor for laboratory-adapted and vaccine strains of MV. CD46 is expressed in all human nucleated cells including epithelial cells (Gerlier and Valentin, 2009). In 2000, human CD150, a signaling lymphocyte activation molecule (SLAM), was identified as the second MV entry receptor for all MV strains including WT (Tatsuo et al., 2000). Expression of CD150 is restricted to activated lymphocytes, dendritic cells (DCs), and macrophages (Delpeut et al., 2012), consistent with the lymphotropism of MV. However, the expression pattern of CD150 does not explain why WT strains of MV infect epithelial cells that do not express CD150. Recently, human nectin-4 (also called poliovirus receptor-related 4, PVRL4) was identified as the third entry receptor for WT strains of MV (Mühlebach et al., 2011; Noyce et al., 2011). Expression of nectin-4 is restricted to the basolateral surface of epithelial cells (Delpeut et al., 2012). Thus, laboratory-adapted and vaccine strains of MV use CD46 and CD150 as entry receptors, and WT strains of MV use CD150 and nectin-4. Initial infection with WT stains of MV *via* CD150 occurs in DCs and alveolar macrophages (AMs) and secondary spreading of MV infection is established in lymphocytes through infected DCs and AMs. Ultimately, MV-infected lymphocytes systemically spread to distal sites including the respiratory tract and then MV infects epithelial cells *via* nectin-4, resulting in release of MV into the airway lumen of the infected lung (Delpeut et al., 2012). C-type lectin DC-SIGN (also called CD209) has an important role for infection of DCs by laboratory-adapted and WT strains of MV (de Witte et al., 2006), although DC-SIGN is dispensable for MV entry. Both attachment and infection of immature DCs with MV are blocked by DC-SIGN inhibitors, suggesting that DC-SIGN is critical for enhancement of CD46/CD150-mediated infection of DCs (de Witte et al., 2006).

Human CD150 transgenic (Tg) and CD150 knock-in mice were generated as MV infection models to study receptor tropism and the immune dynamics of MV (Hahm et al., 2003, 2004; Ohno et al., 2007; Sellin et al., 2006; Shingai et al., 2005; Welstead et al., 2005) and these mice were somehow permissive to MV *in vivo*.

* Corresponding authors at: Department of Microbiology and Immunology, Hokkaido University Graduate School of Medicine, Kita 15, Nishi 7, Kita-ku, Sapporo 060-8638, Japan. Tel.: +81 11 706 7866; fax: +81 11 706 7866.
E-mail addresses: tahiromi@sci.hokudai.ac.jp (H. Takaki), seya-tu@pop.med.hokudai.ac.jp (T. Seya).

http://dx.doi.org/10.1016/j.biocel.2014.05.001
1357-2725/

Systemic infection by WT strains of MV *in vivo* was observed in CD150Tg/*Ifnar*$^{-/-}$ mice, generated by crossing CD150Tg mice with mice having the disrupted IFN receptor 1 (*Ifnar*) gene; the other is CD150Tg/*Stat1*$^{-/-}$ mice, generated by crossing CD150Tg mice with mice knocked out for the signal transduction and activator of transcription 1 (*Stat1*) gene, which is a major signaling molecule for the IFN receptor (Shingai et al., 2005; Welstead et al., 2005). Both models indicate the importance of the IFNAR pathway for restricting MV *in vivo* infection in mice. DCs and AMs are primary targets for MV intranasally inoculated into CD150Tg models (Ferreira et al., 2010), since these cells express CD150 and are located in the lung where host cells firstly encounter MV. Results from mouse models for MV *in vivo* infection reflect *in vitro* high susceptibility of human monocyte-derived DCs (moDCs) to MV. DCs and AMs are the first target cells during early MV infection in monkeys (de Swart et al., 2007; Lemon et al., 2011). All these data indicate that type I IFN produced by DCs and AMs primarily protects hosts from systemic MV infection.

In this review, we summarized the mouse model studies on the host antiviral response to MV infection, which involves both toll-like receptors (TLRs) and retinoic acid-inducible gene (RIG)-I-like receptors (RLRs) in specific DC subsets.

2. Type I IFN-inducing pathways respond to viral RNA

The IFN response, which is the induction of type I IFN-α/β is a major antiviral defense pathway that confers virus resistance to neighboring cells. Previous reports showed that viral RNA is detected by cytoplasmic pattern recognition receptors (PRRs) such as RIG-I and the melanoma differentiation-associated gene 5 (MDA5) (Kawai and Akira, 2009). MDA5 and RIG-I detect long and short dsRNA, respectively (Kato et al., 2008). TLR3 recognizes extracellular double-stranded RNA (dsRNA) in the endosome whereas RIG-I and MDA5 sense cytoplasmic dsRNA (Fig. 1). TLR3 recruits the adaptor, Toll/interleukin-1 receptor (TIR) homology domain-containing adaptor molecule 1 (TICAM-1, also called TRIF) in response to dsRNA and induces type I IFN production. Activation of RLRs is regulated by multiple consecutive processes including dephosphorylation, ubiquitination and oligomerization of RLR (Gack et al., 2007; Wies et al., 2013). The CARD domain of RLRs is phosphorylated by unknown kinases in steady state, prohibiting RLR activation (Wies et al., 2013). Viral infection activates RLRs *via* dephosphorylation by serine–threonine phosphatases PP1α and PP1γ (Wies et al., 2013). The dephosphorylated RLRs provide signals through the mitochondrial antiviral signaling protein (MAVS; also called VISA, Cardif, or IPS-1) to induce type I IFN. Disrupting these adaptor genes results in failure to activate IFN regulatory factor (IRF)-3 and IRF-7, abrogating type I IFN production and antiviral host defense. Virus-derived single-stranded RNA (ssRNA) is recognized by TLR7 and TLR8 which are in the endosome. MyD88-dependent signaling is activated upon viral RNA recognition by TLR7 to induce type I IFNs (Kawai and Akira, 2009). Unlike ubiquitous RLRs, TLR expression is restricted to particular cell types with a different set of TLRs (Table 1) (Edwards et al., 2003). This differential expression pattern of TLRs directs specific sets of cells to respond to particular TLR ligands, which enhance a variety of immune responses.

3. Type I IFN induction in MV-infected murine DCs

Studies in mice with targeted gene deletions provide insight into the mechanisms of type I IFN induction in response to MV infection *in vivo* and *in vitro*. Bone marrow-derived DCs (BMDCs) were used to study MV permissiveness of DCs, initially in CD150Tg mice (Ohno et al., 2007; Shingai et al., 2005; Welstead et al., 2005). Studies using BMDCs from CD150Tg mice in combination with *Mavs*$^{-/-}$, *Irf3*$^{-/-}$/*Irf7*$^{-/-}$, *Ticam1*$^{-/-}$ and *Myd88*$^{-/-}$ mice showed that type I IFN expression in BMDCs completely relied on MAVS but not TICAM-1 and MyD88 (Takaki et al., 2014). Surprisingly, BMDCs derived from CD150Tg/*Irf3*$^{-/-}$/*Irf7*$^{-/-}$ mice produce a detectable IFN-β in response to MV infection, which confers nonpermissiveness to CD150Tg/*Irf3*$^{-/-}$/*Irf7*$^{-/-}$ BMDCs (Takaki et al., 2014). A pharmacological study indicated that MV-derived IFN-β expression partially depended on NF-κB (Takaki et al., 2014). A recent study using West Nile virus showed that IRF3/IRF7 and IRF5 coordinately regulate the type I IFN response in DCs (Lazear et al., 2013). For MV, IRF5 might be a transcription factor for MAVS-dependent and IRF3/IRF7-independent type I IFN induction in BMDCs (Fig. 2).

An *in vivo* MV infection study using a CD150Tg mouse model revealed that MAVS disruption scarcely led MV permissiveness or type I IFN gene expression in the spleen compared to CD150Tg mice (Takaki et al., 2013). *In vitro* infection assays showed that isolated cell subsets of CD11c^{+} DCs, but not T or B cells, mainly produced type I IFN in response to MV infection through a MAVS-independent pathway. Various types of DCs have been identified in mouse secondary lymphoid tissues, including three CD11c^{high} subsets of conventional DCs (cDCs): CD8α^{+}, CD4^{+} and CD4^{-} CD8α^{-} double negative (DN) DCs (Vremec et al., 2000), and one subset of CD11c^{low} plasmacytoid DCs (pDCs) (Asselin-Paturel et al., 2001). These DC subsets express different sets of TLR genes and have distinct functions (Table 1) (Edwards et al., 2003; Luber et al., 2010). Mouse pDCs express most TLRs except TLR3 and therefore respond to a wide range of pathogen-associated molecular patterns including TLR7 ligand (Boonstra et al., 2003; Edwards et al., 2003). CD8α^{+} DCs express high amounts of TLR3, but not TLR7 (Edwards et al., 2003) and mainly participate in poly I:C-induced cross-presentation. Although a CD4^{+} and DN DCs have a similar TLR expression pattern (Edwards et al., 2003), CD4^{+} DCs but not DN DCs express TLR7 protein at low levels (Takaki et al., 2013). Type I IFN expression is induced in CD4^{+} DCs and pDCs, but not CD8α^{+} and DN DCs that are isolated from MAVS-disrupted mice during *in vitro* MV infection (Takaki et al., 2013). This result indicates that type I IFN-inducing pathways in pDC and CD4^{+} DCs are independent of the MAVS pathway. A pharmacological study showed that the MyD88 pathway is involved in a MAVS-independent type I IFN-inducing pathway (Takaki et al., 2013). This result was confirmed using CD150Tg/*Myd88*$^{-/-}$ pDCs, suggesting that TLR7 is responsible for recognition of MV RNA in CD4^{+} and pDCs. Since the RLR-MAVS pathway usually senses endogenous viral RNA in CD4^{+} DCs (Luber et al., 2010), MAVS disruption highlights that the MyD88 pathway participates in initial type I IFN induction in CD4^{+} DCs in MV infection (Fig. 2). However, CD150Tg/*Myd88*$^{-/-}$ mice are not permissive to MV infection *in vivo*, both MyD88 in pDCs and CD4^{+} DCs and MAVS in other cells contribute to protection against systemic MV infection.

Since TLR7 is in the endosome, viral RNA transport to the endosome is required to activate the TLR7/MyD88 pathway. Autophagy is required for the recognition of vesicular stomatitis virus by TLR7 to transport cytosolic viral replication intermediates into the lysosome, leading to type I IFN production in pDCs (Lee et al., 2007) IFN-β mRNA expression is induced in UV-irradiated MV-infected CD150Tg/*Mavs*$^{-/-}$ DCs; however, treatment with an autophagy inhibitor prevented this IFN-β induction (unpublished data). These data suggest that autophagy but not viral replication is required for MV-mediated type I IFN induction *via* TLR7 in MAVS-disrupted murine DCs.

In contrast to BMDCs, type I IFN gene expression is observed in DCs and splenocytes derived from MV-infected CD150Tg/*Mavs*$^{-/-}$ mice, which prevents DCs from MV infection *in vivo* in these mice (Takaki et al., 2013, 2014). RIG-I/MAVS but not TLR7/MyD88 mediates the antiviral response to RNA virus in conventional DCs. The

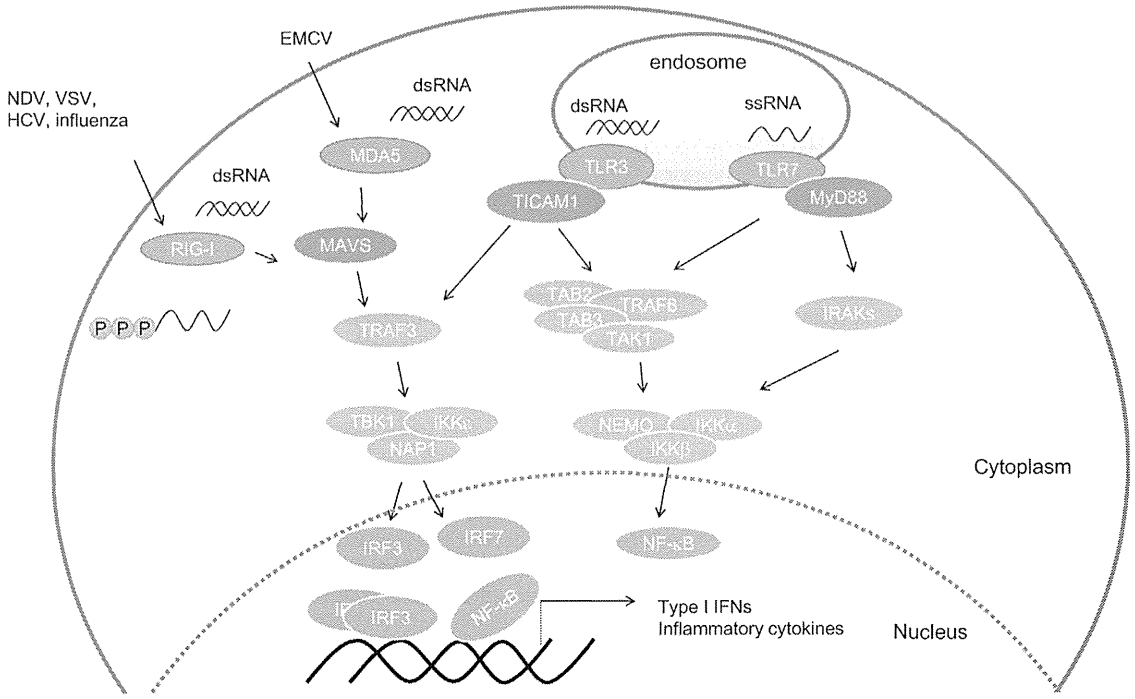

Fig. 1. Recognition of RNA by RLRs and TLRs. Double-stranded RNA (dsRNA) synthesized by RNA virus replication in infected cells is recognized by endosomal TLR3 and cytosolic RIG-I like receptors (RLRs), RIG-I and MDA5. They differentially recognize viral dsRNA products such that long dsRNA chains fit in MDA5, 5′-triphosphates short dsRNA couple with RIG-I and structured RNA activate TLR3 (Tatematsu et al., 2013). The outline of their signaling cascades that lead to the activation of IRF3 and NF-κB is overviewed (Kawai and Akira, 2009). Single-stranded RNA (ssRNA) is recognized by endosomal TLR7, leading to the activation of NF-κB and IKK α/β *via* adaptor protein MyD88. Transcription factor activation resuls in expression of type I IFN and inflammatory cytokines. NDV, newcastle disease virus; SeV, sendai virus; HCV, hepatitis C; EMCV, encephalomyocarditis virus

Table 1
Expression of TLRs in murine and human DC subset.

			TLR1	TLR2	TLR3	TLR4	TLR5	TLR6	TLR7	TLR8	TLR9	TLR10
Mouse	Conventional DCs ($CD11c^{high}$ $B220^{-}$)	$CD4^{+}$	+	+	–	+	+	+	+	–	+	–
		$CD4^{-}CD8\alpha^{-}$	+	+	+/–	+	+	+	+/–	–	+	–
		$CD4^{-}$	+	+	+	+	–	+	–	–	+	–
	Plasmacytoid DCs ($CD11c^{low}$ $B220^{+}$ $PDCA{-}1^{+}$)		+	+	–	+	+/–	+	+	–	+	–
Human	Myeloid DCs ($CD11c^{+}$)		+	+	+	+	+	+	+	+/–	–	+
	Monocyte-derived DCs (moDCs)		+	+	+	+	+	+/–	+/–	+	–	–
	Plasmacytoid DCs ($CD11c^{-}$ $BDCA2^{+}$ $BDCA4^{+}$)		+/–	–	–	–	–	–	+	–	+	+

TLR expression in murine and human DC subset is described in refs (Jarrossay et al., 2001; Kadowaki et al., 2001; Edwards et al., 2003; Luber et al., 2010).

studies using reporter mouse that expresses green fluorescence protein (GFP) under the control of the *Ifn-α6* promoter show that intranasal infection with newcastle disease virus (NDV) induces GFP expression in AMs and cDCs in lung as an initial defense *via* the RLR pathway (Kumagai et al., 2007). Although systemic NDV infection leads to GFP expression in not only pDCs but also cDCs and AMs, the frequency of GFP positive cells is higher in pDCs than in other cells. Thus, the activation of different subsets of DCs would be important to produce type I IFNs in systemic and local RNA virus infection.

Similar to murine DCs, PRRs expression differs with subsets of human DCs (Table 1) (Jarrossay et al., 2001; Kadowaki et al., 2001). In cDCs, MV transcription is required to activate type I IFN response, since UV-irradiated MV is unable to promote IFN-β production (Duhen et al., 2010). Type I IFN induction by pDCs depends on the recognition of MV RNA *via* the endosomal pathway, since UV-irradiated MV infection induces IFN-α production and this induction is cancelled by an endosomal acidification inhibitor in pDCs (Duhen et al., 2010). Although MV can inhibit TLR7 and TLR9-mediated type I IFN induction by MV-V and MV-C proteins in human pDCs (Pfaller and Conzelmann, 2008; Schlender et al., 2005; Yamaguchi et al., 2014), it remains unknown whether MV proteins act as suppressors in murine DCs. Moreover, MV interacts with human DC-SIGN to enhance infection of human DCs (de Witte et al., 2006). However, how MV-H protein binds murine CIRE/DC-SIGN is unknown. The findings in murine DCs may differ from those in human DCs when infected with MV.

4. Type I IFN and cytokines in the context of MV immunosuppression

DCs contribute to MV-induced immunosuppression, including downregulation of costimulatory molecules and inhibition of IL-12 production following lipopolysaccharide stimulation (Coughlin et al., 2013; Hahm et al., 2004, 2007). MV infection suppressed BMDCs development *via* type I IFN that acts through STAT2-dependent signaling but independent of the STAT1 signaling (Hahm et al., 2005). Furthermore, *in vivo* MV infection induces a T helper type 2 response, enhances apoptosis, and induces regulatory T cells (Koga et al., 2010; Sellin et al., 2009). Blocking IL-10 signaling prevents MV-induced immunosuppression in CD150 knock-in mice, indicating that IL-10 participates in immunosuppression (Koga et al., 2010). In addition, high amounts of IL-10 are produced in $CD4^{+}$ T cells obtained from MV-infected CD150Tg mice (Takaki

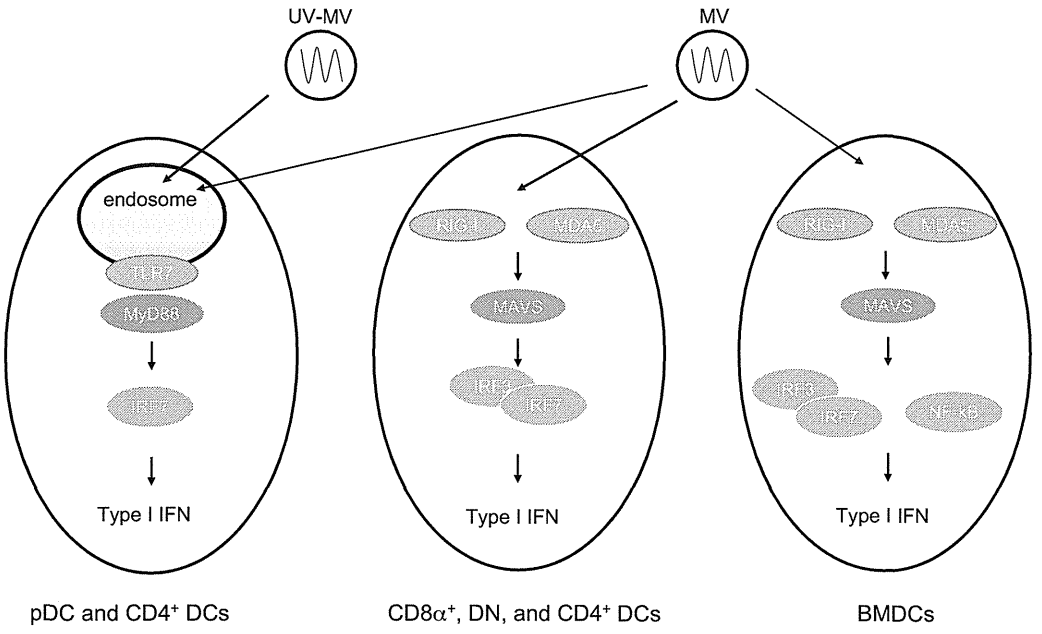

Fig. 2. Recognition of MV RNA in mouse DC subsets. DC subsets have their own viral RNA sensors to induce type I IFN. MV specifically infects these DC subsets. The ways for IFN induction in each DC subset are shown schematically. UV-MV; UV-irradiated MV

et al., 2014). In early infection by lymphocytic choriomeningitis virus (LCMV), type I IFN is produced *via* the TLR7/MyD88 pathway in pDCs. MDA5/MAVS-mediated type I IFN induction in other cells is required for sustained type I IFN responses to acute and chronic LCMV infection (Wang et al., 2012). Thus, different sources of type I IFN and signaling pathways affect immune responses to viral infection. Besides IL-10, IL-12 and type I IFN, other cytokines and signaling molecules affect MV-mediated immunomodulation. Further analysis is needed to clarify the function of DCs that modulate MV-induced immunosuppression.

Acknowledgements

We are grateful to Dr. M. Takeda (National Institute of Infectious Diseases, Japan) for fruitful discussions. This work was supported in part by Grants-in-Aid from the Ministry of Education, Science, and Culture (Specified Project for 'Carcinogenic Spiral') and the Ministry of Health, Labor, and Welfare of Japan, and by the Program of Founding Research Centers for Emerging and Reemerging Infectious Diseases (Host factors determining tropism and pathogenicity of zoonoses in association with innate immune system) and Japan Society for the promotion of Science Fellows (21-1368).

References

Asselin-Paturel C, Boonstra A, Dalod M, Durand I, Yessaad N, Dezutter-Dambuyant C, et al. Mouse type I IFN-producing cells are immature APCs with plasmacytoid morphology. Nat Immunol 2001;2:1144–50.

Boonstra A, Asselin-Paturel C, Gilliet M, Crain C, Trinchieri G, Liu YJ, et al. Flexibility of mouse classical and plasmacytoid-derived dendritic cells in directing T helper type 1 and 2 cell development: dependency on antigen dose and differential toll-like receptor ligation. J Exp Med 2003;197:101–9.

Coughlin MM, Bellini WJ, Rota PA. Contribution of dendritic cells to measles virus induced immunosuppression. Rev Med Virol 2013;23:126–38.

de Swart RL, Ludlow M, de Witte L, Yanagi Y, van Amerongen G, McQuaid S, et al. Predominant infection of CD150+ lymphocytes and dendritic cells during measles virus infection of macaques. PLoS Pathog 2007;3:e178.

de Witte L, Abt M, Schneider-Schaulies S, van Kooyk Y, Geijtenbeek TB. Measles virus targets DC-SIGN to enhance dendritic cell infection. J Virol 2006;80:3477–86.

Delpeut S, Noyce RS, Siu RW, Richardson CD. Host factors and measles virus replication. Curr Opin Virol 2012;2:773–83.

Duhen T, Herschke F, Azocar O, Druelle J, Plumet S, Delprat C, et al. Cellular receptors, differentiation and endocytosis requirements are key factors for type I IFN response by human epithelial, conventional and plasmacytoid dendritic infected cells by measles virus. Virus Res 2010;152:115–25.

Edwards AD, Diebold SS, Slack EM, Tomizawa H, Hemmi H, Kaisho T, et al. Toll-like receptor expression in murine DC subsets: lack of TLR7 expression by CD8 alpha+ DC correlates with unresponsiveness to imidazoquinolines. Eur J Immunol 2003;33:827–33.

Ferreira CS, Frenzke M, Leonard VH, Welstead GG, Richardson CD, Cattaneo R. Measles virus infection of alveolar macrophages and dendritic cells precedes spread to lymphatic organs in transgenic mice expressing human signaling lymphocytic activation molecule (SLAM, CD150). J Virol 2010;84:3033–42.

Gack MU, Shin YC, Joo CH, Urano T, Liang C, Sun L, et al. TRIM25 RING-finger E3 ubiquitin ligase is essential for RIG-I-mediated antiviral activity. Nature 2007;446:916–20.

Gerlier D, Valentin H. Measles virus interaction with host cells and impact on innate immunity. Curr Top Microbiol Immunol 2009;329:163–91.

Hahm B, Arbour N, Naniche D, Homann D, Manchester M, Oldstone MB. Measles virus infects and suppresses proliferation of T lymphocytes from transgenic mice bearing human signaling lymphocytic activation molecule. J Virol 2003;77:3505–15.

Hahm B, Arbour N, Oldstone MB. Measles virus interacts with human SLAM receptor on dendritic cells to cause immunosuppression. Virology 2004;323:292–302.

Hahm B, Cho JH, Oldstone MB. Measles virus-dendritic cell interaction via SLAM inhibits innate immunity: selective signaling through TLR4 but not other TLRs mediates suppression of IL-12 synthesis. Virology 2007;358:251–7.

Hahm B, Trifilo MJ, Zuniga EI, Oldstone MB. Viruses evade the immune system through type I interferon-mediated STAT2-dependent, but STAT1-independent, signaling. Immunity 2005;22:247–57.

Jarrossay D, Napolitani G, Colonna M, Sallusto F, Lanzavecchia A. Specialization and complementarity in microbial molecule recognition by human myeloid and plasmacytoid dendritic cells. Eur J Immunol 2001;31:3388–93.

Kadowaki N, Ho S, Antonenko S, Malefyt RW, Kastelein RA, Bazan F, et al. Subsets of human dendritic cell precursors express different toll-like receptors and respond to different microbial antigens. J Exp Med 2001;194:863–9.

Kato H, Takeuchi O, Mikamo-Satoh E, Hirai R, Kawai T, Matsushita K, et al. Length-dependent recognition of double-stranded ribonucleic acids by retinoic acid-inducible gene-I and melanoma differentiation-associated gene 5. J Exp Med 2008;1601–10, J205.

Kawai T, Akira S. The roles of TLRs, RLRs and NLRs in pathogen recognition. Int Immunol 2009;21:317–37.

Koga R, Ohno S, Ikegame S, Yanagi Y. Measles virus-induced immunosuppression in SLAM knock-in mice. J Virol 2010;84:5360–7.

Kumagai Y, Takeuchi O, Kato H, Kumar H, Matsui K, Morii E, et al. Alveolar macrophages are the primary interferon-alpha producer in pulmonary infection with RNA viruses. Immunity 2007;27:240–52.

Lazear HM, Lancaster A, Wilkins C, Suthar MS, Huang A, Vick SC, et al. IRF-3, IRF-5, and IRF-7 coordinately regulate the type I IFN response in myeloid dendritic cells downstream of MAVS signaling. PLoS Pathog 2013;9:e1003118.

Lee HK, Lund JM, Ramanathan B, Mizushima N, Iwasaki A. Autophagy-dependent viral recognition by plasmacytoid dendritic cells. Science 2007;315:1398–401.

Lemon K, de Vries RD, Mesman AW, McQuaid S, van Amerongen G, Yüksel S, et al. Early target cells of measles virus after aerosol infection of non-human primates. PLoS Pathog 2011;7:e1001263.

Luber CA, Cox J, Lauterbach H, Fancke B, Selbach M, Tschopp J, et al. Quantitative proteomics reveals subset-specific viral recognition in dendritic cells. Immunity 2010;32:279–89.

Mühlebach MD, Mateo M, Sinn PL, Prüfer S, Uhlig KM, Leonard VH, et al. Adherens junction protein nectin-4 is the epithelial receptor for measles virus. Nature 2011;480:530–3.

Noyce RS, Bondre DG, Ha MN, Lin LT, Sisson G, Tsao MS, et al. Tumor cell marker PVRL4 (nectin 4) is an epithelial cell receptor for measles virus. PLoS Pathog 2011;7:e1002240.

Ohno S, Ono N, Seki F, Takeda M, Kura S, Tsuzuki T, et al. Measles virus infection of SLAM (CD150) knockin mice reproduces tropism and immunosuppression in human infection. J Virol 2007;81:1650–9.

Pfaller CK, Conzelmann KK. Measles virus V protein is a decoy substrate for IkappaB kinase alpha and prevents Toll-like receptor 7/9-mediated interferon induction. J Virol 2008;82:12365–73.

Schlender J, Hornung V, Finke S, Günthner-Biller M, Marozin S, Brzózka K, et al. Inhibition of toll-like receptor 7- and 9-mediated alpha/beta interferon production in human plasmacytoid dendritic cells by respiratory syncytial virus and measles virus. J Virol 2005;79:5507–15.

Sellin CI, Davoust N, Guillaume V, Baas D, Belin MF, Buckland R, et al. High pathogenicity of wild-type measles virus infection in CD150 (SLAM) transgenic mice. J Virol 2006;80:6420–9.

Sellin CI, Jégou JF, Renneson J, Druelle J, Wild TF, Marie JC, et al. Interplay between virus-specific effector response and Foxp3 regulatory T cells in measles virus immunopathogenesis. PLoS ONE 2009;4:e4948.

Shingai M, Inoue N, Okuno T, Okabe M, Akazawa T, Miyamoto Y, et al. Wild-type measles virus infection in human CD46/CD150-transgenic mice: CD11c-positive dendritic cells establish systemic viral infection. J Immunol 2005;175:3252–61.

Takaki H, Honda K, Atarashi K, Kobayashi F, Ebihara T, Oshiumi H, et al. MAVS-dependent IRF3/7 bypass of interferon β-induction restricts the response to measles infection in CD150Tg mouse bone marrow-derived dendritic cells. Mol Immunol 2014;57:100–10.

Takaki H, Takeda M, Tahara M, Shingai M, Oshiumi H, Matsumoto M, et al. The MyD88 pathway in plasmacytoid and CD4+ dendritic cells primarily triggers Type I IFN production against measles virus in a mouse infection model. J Immunol 2013;191:4740–7.

Tatematsu M, Nishikawa F, Seya T, Matsumoto M. Toll-like receptor 3 recognizes incomplete stem structures in single-stranded viral RNA. Nat Commun 2013;4:1833.

Tatsuo H, Ono N, Tanaka K, Yanagi YSLAM. (CDw150) is a cellular receptor for measles virus. Nature 2000;406:893–7.

Vremec D, Pooley J, Hochrein H, Wu L, Shortman K. CD4 and CD8 expression by dendritic cell subtypes in mouse thymus and spleen. J Immunol 2000;164:2978–86.

Wang Y, Swiecki M, Cella M, Alber G, Schreiber RD, Gilfillan S, et al. Timing and magnitude of type I interferon responses by distinct sensors impact CD8T cell exhaustion and chronic viral infection. Cell Host Microbe 2012;11:631–42.

Welstead GG, Iorio C, Draker R, Bayani J, Squire J, Vongpunsawad S, et al. Measles virus replication in lymphatic cells and organs of CD150 (SLAM) transgenic mice. Proc Natl Acad Sci U S A 2005;102:16415–20.

Wies E, Wang MK, Maharaj NP, Chen K, Zhou S, Finberg RW, et al. Dephosphorylation of the RNA sensors RIG-I and MDA5 by the phosphatase PP1 is essential for innate immune signaling. Immunity 2013;38:437–49.

Yamaguchi M, Kitagawa Y, Zhou M, Itoh M, Gotoh B. An anti-interferon activity shared by paramyxovirus C proteins: inhibition of toll-like receptor 7/9-dependent alpha interferon induction. FEBS Lett 2014;588:28–34.

JBC Papers in Press. Published on December 30, 2014 as Manuscript M114.602540
The latest version is at http://www.jbc.org/cgi/doi/10.1074/jbc.M114.602540

Dysregulation of retinoic acid receptor diminishes hepatocyte permissiveness to hepatitis B virus infection through modulation of NTCP expression

Senko Tsukuda[1,2], Koichi Watashi[1]*, Masashi Iwamoto[1], Ryosuke Suzuki[1], Hideki Aizaki[1], Maiko Okada[3], Masaya Sugiyama[4], Soichi Kojima[2], Yasuhito Tanaka[5], Masashi Mizokami[4], Jisu Li[6], Shuping Tong[6], Takaji Wakita[1]

[1]Department of Virology II, National Institute of Infectious Diseases, Tokyo, 162-8640, Japan, [2]Micro-signaling Regulation Technology Unit, RIKEN Center for Life Science Technologies, Wako, 351-0198, Japan. [3]Department of Translational Oncology, St. Marianna University School of Medicine, Kawasaki, 216-8511, Japan, [4]The Research Center for Hepatitis and Immunology, National Center for Global Health and Medicine, Ichikawa, 272-8516, Japan, [5]Department of Virology and Liver Unit, Nagoya City University Graduate School of Medicinal Sciences, Nagoya, 467-8601, Japan, [6]Liver Research Center Rhode Island Hospital, Warren Alpert School of Medicine, Brown University, Province, Rhode Island, 02912, USA.

Running Title: Retinoids reduced HBV susceptibility by downregulating NTCP

***Address correspondence to:** Koichi Watashi, Ph.D.
Department of Virology II, National Institute of Infectious Diseases
1-23-1 Toyama, Shinjuku-ku, Tokyo, 162-8640, Japan
Tel: +81-3-5285-1111; Fax: +81-3-5285-1161
E-mail: kwatashi@nih.go.jp

Keywords: hepatitis virus, transporter, retinoid, transcription, chemical biology, HBV, infection, RAR, permissive, NTCP

Background: Host factors regulating hepatitis B virus (HBV) entry receptors are not well defined.
Results: Chemical screening identified that retinoic acid receptor (RAR) regulates sodium taurocholate cotransporting polypeptide (NTCP) expression and supports HBV infection.
Conclusion: RAR regulates NTCP expression, and thereby supports HBV infection.
Significance: RAR regulation of NTCP can be a target for preventing HBV infection.

Abstract

Sodium taurocholate cotransporting polypeptide (NTCP) is an entry receptor for hepatitis B virus (HBV) and is regarded as one of the determinants that confer HBV permissiveness to host cells. However, how host factors regulate the ability of NTCP to support HBV infection is largely unknown. We aimed to identify the host signaling that regulated NTCP expression and, thereby, permissiveness to HBV. Here, a cell-based chemical screening method identified that Ro41-5253 decreased host susceptibility to HBV infection. Pretreatment with Ro41-5253 inhibited the viral entry process without affecting HBV replication. Intriguingly, Ro41-5253 reduced expression of both NTCP mRNA and protein. We found that retinoic acid receptor (RAR) regulated the promoter activity of the human NTCP (hNTCP) gene, and that Ro41-5253 repressed the hNTCP promoter by antagonizing RAR. RAR recruited to the hNTCP promoter region, and nt -112 to -96 of the hNTCP was suggested to be critical for RAR-mediated transcriptional activation. HBV susceptibility was decreased in pharmacologically RAR-inactivated cells. CD2665 showed a stronger anti-HBV potential and disrupted the spread of HBV infection that was achieved by continuous reproduction of whole HBV life cycle. In addition, this mechanism was significant for drug development, as antagonization of RAR blocked infection of multiple HBV genotypes and also a clinically relevant HBV mutant which was resistant to nucleoside analogs. Thus, RAR is crucial for regulating NTCP expression which determines permissiveness to HBV infection. This is the first demonstration showing host regulation of NTCP to support HBV infection.

Introduction

Hepatitis B virus (HBV) infection is a major public health problem, as the virus chronically infects approximately 240 million people worldwide (1-3). Chronic HBV infection elevates the risk for developing liver cirrhosis and hepatocellular carcinoma (4-6). Currently, two classes of antiviral agents are available to combat chronic HBV infection. First, interferon (IFN)-based drugs including IFNα and pegylated-IFNα modulate host immune function and/or directly inhibit HBV replication in hepatocytes (7,8). However, the antiviral efficacy of IFN-based drugs is restricted to less than 40% (9,10). Second, nucleos(t)ide analogues including lamivudine (LMV), adefovir, entecavir (ETV), tenofovir and telbivudine suppress HBV by inhibiting the viral reverse transcriptase (11,12). Although they can provide significant clinical improvement, long-term therapy with nucleos(t)ide analogues often results in the selection of drug resistant mutations in the target gene, which limits the treatment outcome. For example, in patients treated with ETV, at least three mutations can arise in the reverse transcriptase sequence at of the polymerase L180M, M204V plus either one of T184, S202 or M250 codon changes to acquire drug resistance (13). Therefore, development of new anti-HBV agents targeting other molecules requires elucidation of the molecular mechanisms underlying the HBV life cycle.

HBV infection of hepatocytes involves multiple steps. The initial viral attachment to the host cell surface starts with a low affinity binding involving heparan sulfate proteoglycans, and the following viral entry is mediated by a specific interaction between HBV and its host receptor(s) (14). Recently, sodium taurocholate cotransporting polypeptide (NTCP) was reported as a functional receptor for HBV (15). NTCP interacts with HBV large surface protein (HBs) to mediate viral attachment and the subsequent entry step. NTCP, also known as solute carrier protein 10A1 (SLC10A1), is physiologically a sodium-dependent transporter for bile salts located on the basolateral membrane of hepatocytes (16). In the liver, hepatocytes take up bile salts from the portal blood and secrete them into bile for enterohepatic

circulation, and NTCP-mediated uptake of bile salts into hepatocytes occurs largely in a sodium-dependent manner. Although NTCP is abundant in freshly isolated primary hepatocytes, it is weakly or no longer expressed in most cell lines such as HepG2 and Huh-7, and these cells rarely support HBV infection (17,18). In contrast, primary human hepatocytes, primary tupaia hepatocyte and differentiated HepaRG cells, which are susceptible to HBV infection, express significant levels of NTCP (19). Thus, elucidation of the regulatory mechanisms for NTCP gene expression is important for understanding the HBV susceptibility of host cells as well as for developing a new anti-HBV strategy. HBV entry inhibitors are expected to be useful for preventing *de novo* infection after liver transplantation, for post-exposure prophylaxis, or vertical transmission by short-term treatment (20,21).

In this study, we used a HepaRG-based HBV infection system to screen for small molecules capable of decreasing HBV infection. We found that pretreatment of host cells with Ro41-5253 reduced HBV infection. Ro41-5253 reduced NTCP expression by repressing the promoter activity of the human NTCP (hNTCP) gene. Retinoic acid receptor (RAR) played a crucial role in regulating the promoter activity of hNTCP, and Ro41-5253 antagonized RAR to reduce NTCP transcription and consequently HBV infection. This and other RAR inhibitors showed anti-HBV activity against different genotypes and an HBV nucleoside analog-resistant mutant, and moreover inhibited the spread of HBV. This study clarified one of the mechanisms for gene regulation of NTCP to support HBV permissiveness, and also suggests a novel concept whereby manipulation of this regulation machinery can be useful for preventing HBV infection.

Experimental Procedures

Regents

Heparin was obtained from Mochida Pharmaceutical. Lamivudine, cyclosporin A, all-trans retinoic acid (ATRA), and TO901317 were obtained from Sigma. Entecavir was obtained from Santa Cruz Biotechnology. Ro41-5253 was obtained from Enzo life sciences. PreS1-lipopeptide and FITC-labeled preS1 were synthesized by CS bio. IL-1b was purchased from Peprotech. CD2665, BMS195614, BMS493, and MM11253 were purchased from Tocris Bioscience.

Cell culture

HepaRG cells (BIOPREDIC) and primary human hepatocytes (Phoenixbio) were cultured as described previously (19). HepG2 and HepAD38 cells (kindly provided by Dr. Christoph Seeger at Fox Chase Cancer Center) (22), were cultured with DMEM/F-12+GlutaMax (Invitrogen) supplemented with 10 mM HEPES (Invitrogen), 200 units/ml penicillin, 200 μg/ml streptomycin, 10% FBS, and 5 μg/ml insulin. HuS-E/2 cells (kindly provided by Dr. Kunitada Shimotohno at National Center for Global Health and Medicine) were cultured as described previously (23).

Plasmid construction

phNTCP-Gluc, pTK-Rluc was purchased from Genecopoeia and Promega, respectively. pRARE-Fluc was generated as described (25). For constructing phNTCP-Gluc carrying a mutation in a putative RARE (nt -491 to -479), the DNA fragments were amplified by PCR using phNTCP-Gluc as a template with primer sets F1; 5'-CAGATCTTGGAATTCCCAAAATC-3' and 5'-GAGGGGATGTGTCCATTGAAATGTTAATGGGAGCTGAGAGGATGCCAGTATCCTCCCT-3', and with primer sets 5'-CTCTCAGCTCCCATTAACATTTCAATGGACACATCCCCTCCTGGAGGCCAGTGACATT-3' and R6: 5'-CTCGGTACCAAGCTTTCCTTGTT-3'. The resultant products were further amplified by PCR with F1 and R6, and then inserted into the EcoRI/HindIII sites of phNTCP-Gluc to generate phNTCP Mut(-491~-479)-Gluc. Other promoter mutants were prepared by the same method using the primer sets, F1 and 5'-GTGGGTTATCATTTGTTTCCCGAAAACATTAGAGTGAAAGGAGCTGGGTGTTGCCTTTGG-3', 5'-TCCTTTCACTCTAATGTTTTCGGGAAACAAATGATAACCCACTGGACATGGGGAGGGCAC-3' and R6 for -368~-356; F1 and 5'-AATCTAGGTCCAGCCTATTTAAGTCCCTAAATTTCCTTTTCCCAGCTCCGCTCTTGATTCCTT-3', 5'-CTGGGAAAAGGAAATTTAGGGACTTAAAT

AGGCTGGACCTAGATTCAGGTGGGCCCTG GGCAG-3' and R6 for -274 ~ -258; F1 and 5'-TTCTGGGCTTATTTCTATATTTTGCAATCCA CTGAGTGTGCCTCATGGGCATTCATTC-3', 5'-CACACTCAGTGGATTGCAAAATATAGAAA TAAGCCCAGAAGCAGCAAAGTGACAAGGG -3' and R6 for -179 ~ -167; F1 and 5'-AGCTCTCCCAAGCTCAAAGATAAATGCTA GTTTCCTGGGTGCTACTTGTACTCCTCCCTT GTC-3', 5'-GTAGCACCCAGGAAACTAGCATTTATCTTT GAGCTTGGGAGAGCTAGGGCAGGCAGATA AGGT-3' and R6 for -112 ~ -96, respectively. For constructing hNTCP promoter carrying these five mutations (5-Mut), five DNA segments were amplified using the primers as follows: for segment 1, F1 and 5'- GAGGGGATGTGTCCATGACC-3'; for segment 2, 5'-AGCTCCTTTCACTCTCATGGGT-3' and 5'-TCCTTTTCCCAGCTCCGC-3'; for segment 3, 5'-GAGCTGGGAAAAGGAGCTGC-3' and 5'-CCACTGAGTGTGCCTCATGG-3'; for segment 4, 5'- AGGCACACTCAGTGGAGGG-3' and 5'-CTGGGTGCTACTTGTACTCCTCC-3'; for segment 5, 5'-CAAGTAGCACCCAGGAATCCA-3' and R6. For producing a deletion construct for hNTCP promoter, phNTCP (-53~+108)-Gluc, DNA fragment was amplified using the primer sets 5'-GGTGAATTCTGTTCCTCTTTGGGGCGACAG C-3' and 5'-GGTGGTAAGCTTTCCTTGTTC TCCGGCTGACTCC-3' and then inserted into the EcoRI and HindIII sites of phNTCP-Gluc.

HBV preparation and infection

HBV was prepared and infected as described (19). HBV used in this study was mainly derived from HepAD38 cells (22). For Fig. 6A-E, we used concentrated (approximately 200-fold) media of HepG2 cells transfected with an expression plasmid for either HBV genotype A, B, C, D, or genotype C carrying mutations at L180M, S202G, and M204V [HBV/Aeus, HBV/Bj35s, HBV/C-AT, HBV/D-IND60, or HBV/C-AT(L180M/S202G/M204V)] (24), and infected into the cells at 2000 GEq/cell in the presence of 4% PEG8000 at 37 °C for 16 h as previously described (19). HBV for Fig. 6F (genotype C) was purchased from Phoenixbio.

Real time PCR and RT-PCR

Real time PCR for detecting HBV DNAs and cccDNA was performed as described (19). RT-PCR detection of mRNAs for NTCP, ASBT, SHP, and GAPDH was performed with one step RNA PCR kit (TaKaRa) following the manufacturer's protocol with primer set 5'-AGGGAGGAGGTGGCAATCAAGAGTGG-3' and 5'-CCGGCTGAAGAACATTGAGGCACTGG-3' for NTCP, 5'- GTTGGCCTTGGTGATGTTCT-3' and 5'- CGACCCAATAGGCCAAGATA-3' for ASBT, 5'- CAGCTATGTGCACCTCATCG-3' and 5'- CCAGAAGGACTCCAGACAGC-3' for SHP, and 5' -CCATGGAGAAGGCTGGGG-3' and 5'-CAAAGTTGTCATGGATGACC-3' for GAPDH, respectively.

Immunofluorescence analysis

Immunofluorescence was conducted essentially as described (25) using an anti-HBc antibody (DAKO, #B0586) at a dilution of 1:1,000.

Detection of HBs and HBe antigens

HBs and HBe antigens were detected by ELISA and chemiluminescence immunoassay, respectively, as described (19).

MTT assay

The MTT cell viability assay was performed as described previously (19).

Southern blot analysis

Isolation of cellular DNA and southern blot analysis to detect HBV DNAs were performed as described previously (19).

Immunoblot Analysis

Immunoblot analysis was performed as described previously (26,27). Anti-NTCP (Abcam) (1:2000 dilution), anti-RARα (Santa Cruz Biotechnology) (1:6000 dilution), anti-RARβ (sigma) (1:6000 dilution), anti-RARγ (abcam) (1:2000 dilution), anti-RXRα (Santa Cruz Biotechnology) (1:8000 dilution), and anti-actin (Sigma) (1:5000 dilution) antibodies were used for primary antibodies.

Flow cytometry

1 x 10^6 primary human hepatocytes were incubated for 30 min with a 1:50 dilution of anti-NTCP Ab (Abcam), then washed and incubated with a dye-labeled secondary Ab (Alexa Fluor 488, Invitrogen) at 1:500 dilution in the dark. Staining and washing were carried out at 4 °C in PBS supplemented with 0.5% bovine serum albumin and 0.1% sodium azide. The signals were analyzed with Cell Sorter SH8000 (SONY).

FITC-preS1 peptide-binding assay

Attachment of preS1 peptide with host cells was examined by preS1-binding assay essentially as described previously (28). HepaRG cells treated with or without Ro41-5253 (28) for 24 h or unlabeled preS1 peptide for 30 min were incubated with 40 nM FITC-labeled preS1 peptide (FITC-preS1) at 37°C for 30 min. After washing the cells twice with culture medium and once with phosphate-buffer saline (PBS), the cells were fixed with 4% paraformaldehyde. Then, the cells were treated with 4% Block Ace (DS Pharma Biomedical) containing DAPI for 30 min.

Reporter assay

HuS-E/2 cells were transfected with phNTCP-Gluc (GeneCopoeia), a reporter plasmid carrying the NTCP promoter sequence upstream of the Gaussia luciferase (Gluc) gene, and pSEAP (GeneCopoeia), expressing the secreted alkaline phosphatase (SEAP) gene, together with or without expression plasmids for RARα, RARβ, RARγ with RXRα using lipofectamine 2000 (Invitrogen). At 24 h posttransfection, cells were stimulated with the indicated compounds for further 24 h. The activities for Gluc as well as for SEAP were measured using a Secrete-Pair Dual Luminescence Assay Kit (GeneCopoeia) according to the manufacturer's protocol, and Gluc values normalized by SEAP are shown.

pRARE-Fluc, carrying three tandem repeats of RAR binding elements upstream of Firefly luciferase (Fluc) and pTK-Rluc (Promega), which carries herpes simplex virus thymidine kinase promoter expressing Renilla luciferase (Rluc) (25), were used in dual luciferase assays for detecting Fluc and Rluc. Fluc and Rluc were measured with Dual-Luciferase Reporter Assay System (Promega) according to the manufacture's protocol, and Fluc activities normalized by Rluc are shown.

For evaluating HBV transcription in Fig. 2B, we used a reporter construct carrying HBV enhancer I, II, and core promoter (nt 1039-1788) ("Enh I+II"), that carrying enhancer II and core promoter (nt 1413-1788) ("Enh II") that are derived from a genotype D HBV in HepG2.2.15 cells, which was inserted into pGL4.28 vector (Promega), and pGL3 promoter vector (Promega), which carries SV40 promoter ("SV40") as a control.

Chromatin immunoprecipitation (ChIP) assay

ChIP assay was performed using a Pierce Agarose ChIP Kit (Thermo Fisher Scientific) according to the manufacturer's instructions. Huh7-25 cells transfected with phNTCP-Gluc together with or without expression plasmids for FLAG-tagged RARα and for RXRα were treated with 5 μg/ml actinomycin D for 2 h. The cells were then washed and treated with or without 2 μM ATRA for 60 min. Formaldehyde cross-linked cells were lyzed, digested with micrococcal nuclease, immunoprecipitated with anti-FLAG antibody (Sigma) or normal IgG. Input samples were also recovered without immunoprecipitation. DNA recovered from the immunoprecipitated or the input samples was amplified with primers 5'-CCCAGGGCCCACCTGAATCTA-3' and 5'-TAGATTCAGGTGGGCCCTGGG-3' for detection of NTCP.

Results

Anti-HBV activity of Ro41-5253

We searched for small molecules capable of decreasing HBV infection in a cell-based chemical screening method using HBV-susceptible HepaRG cells (29). As a chemical library, we used a set of compounds of which bioactivity is already characterized (19). HepaRG cells were pretreated with compounds and then further incubated with HBV inoculum in the presence of compounds for 16 h (Fig. 1A). After removing free HBV and compounds by washing, the cells were cultured for an additional 12 days without compounds. For robust screening, HBV infection was monitored by ELISA quantification of HBs antigen secreted from the infected cells at 12 days postinfection. This screening revealed that HBs was significantly reduced by treatment with Ro41-5253 (Fig. 1B) as well as heparin, a competitive viral attachment